Context and literature review

Contents

1.1 Frontal impact accidents

The road deaths in the European Union in 2001 were of 55 000. The EU [1] set a target to reduce road fatalities by 50 % by 2010 compared to 2001 levels. Road mortality have been cut by 43 % in the EU leading to 32 000 deaths for the year 2010 according to ETSC [2] (ETSC 2015). This is equivalent to 102 000 less deaths in the EU during this period. In order to keep improving road safety, the commitment has been renewed for 2020 compared to 2010 levels, that is the objective is to have no more than 16 000 road deaths across the EU in 2020. Figure 1.1 shows the results of this policy for the years 2000 to 2014 along with the projection for 2020. This reduction is estimated to saving 182 billion Euro as societal cost.

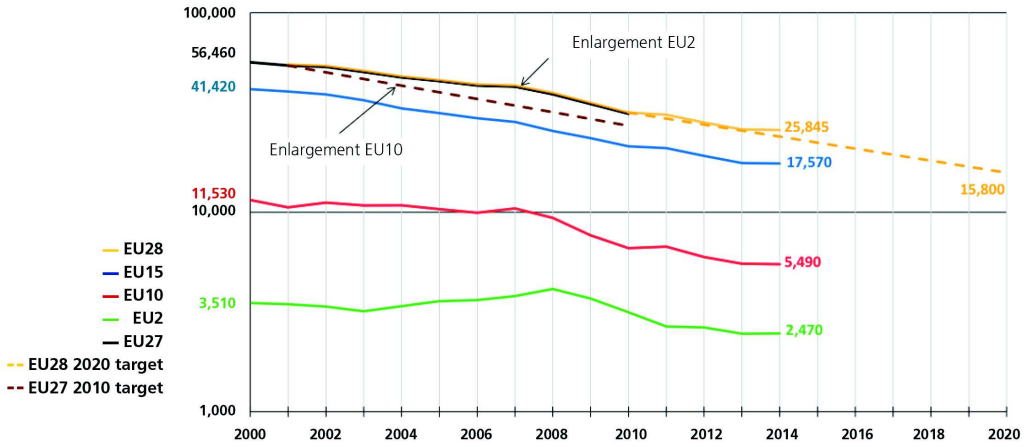

Figure 1.1 – Reduction in road deaths since 2000 in Europe with logarithmic scale (ETSC 2015)
EU15: Austria, Belgium, Denmark, Finland, France, Germany, Greece, Ireland, Italy, Luxembourg, Netherlands, Portugal, Spain, Sweden, United Kingdom
EU10: Cyprus, Czech Republic, Estonia, Hungary, Latvia, Lithuania, Malta, Poland, Slovakia and Slovenia
EU2: Bulgaria and Romania
EU27: EU15 + EU10 + EU2
EU28: EU27 + Croatia

One can also note that the deaths reduction took place despite a constant growth of road traffic as seen on Figure 1.2 according to ETSC 2003. Figure 1.2a presents the fatality rate that is the number of deaths divided by the number of kilometres driven by motor vehicles (in billions) each year in the EU. Figure 1.2b shows the road traffic estimated by the number of kilometres driven by motor vehicles each year in the EU.

Reducing the number of road deaths involves improving many factors such as public policies, regulations, infrastructures and crash performance of vehicles. In order to investigate deeper how to protect the occupants of a vehicle in case of a crash, the occurrence and severity of injuries in case of a crash needs to be considered.

1. European Union
2. European Transport Safety Council

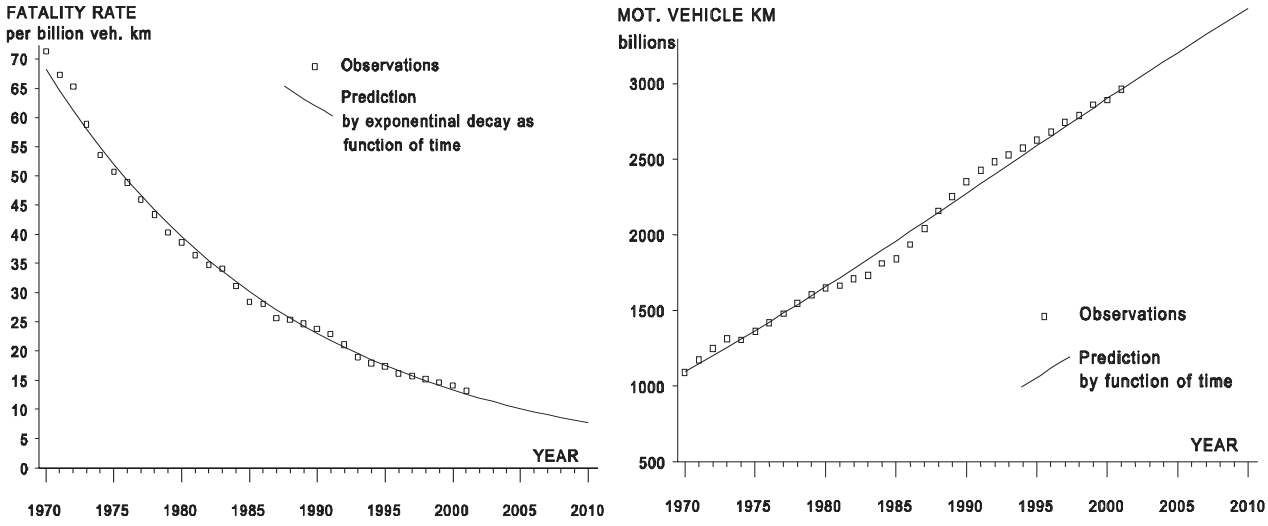

(a) Fatality rate decay

(b) Road traffic growth

Figure 1.2 – Fatality rate and road traffic in Europe (ETSC 2003)

1.1.1 Accidentology

Epidemiological studies analyse car accident databases in order to understand what are the main injury causes to the occupants and to analyse their frequency and severity. Klinich et al. 2010 reported that there is 1.5 times more injuries in frontal impact than in side impact. Rudd et al. 2009 reported that 43 % of occupant fatalities appeared in frontal crashes, making it the impact case creating the more fatalities.

Regarding the abdomen, Elhagediab and Rouhana 1998 demonstrated that the proportion of injuries to the abdomen increases with the injury severity (Table 1.1). This shows that approximately 20 % of the critical injuries are abdominal injuries. Lee and Yang 2002 made similar observations, the abdomen representing the 7th body region in terms of total injuries but the 3rd when looking at the proportion of severe injuries per body region (AIS [3] 3 and more). Yaguchi et al. 2011 also mentioned the abdomen as the 3rd body region in terms of fatalities after the thorax and the head and the 1st by fatality rate (fatalities divided by the sum of all injuries). This puts the abdomen as one of the important body regions to be protected, along with the chest and the head. Martin et al. 2010 described that rear occupants are 1.9 times as likely to sustain abdomen injuries than drivers and 1.5 time than front passengers. Couturier et al. 2007 also stated that rear occupants face a 2.5 time more important abdomen injury risk than front occupants. In each of the two studies, abdomen is the body region that shows the most difference between front and rear occupants for injury risk. There is therefore a benefit for reducing the inequality between car occupants to improve abdomen protection. This has also been highlighted by Frampton et al. 2012, rear occupants sustaining more abdominal injuries (Figure 1.3a) to most of the organs (Figure 1.3b).

3. Abbreviated Injury Scale

	AIS ≥ 3	AIS ≥ 4	AIS ≥ 5
Head	27.8%	35.3%	34.1%
Neck	3.4%	1.8%	2.2%
Chest	37.6%	46.3%	43.3%
Abdomen	8.0%	16.5%	20.5%
Femur	23.2%	0.2%	0.0%
Total	100%	~100%	~100%

Table 1.1 – Injury proportions for body regions depending on injury severity (Elhagediab and Rouhana 1998)

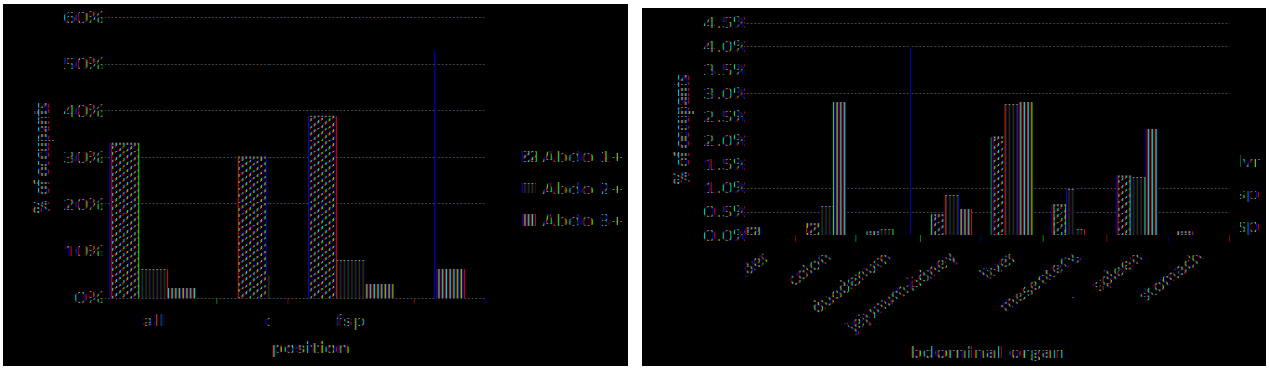

(a) Abdominal injury severity

(b) Abdominal organs injury rates

Figure 1.3 – Abdomen injuries depending on occupant position (Frampton et al. 2012)
dvr: driver, fsp: front seat passenger, rsp: rear seat passenger

1.1.2 Regulation on car passengers protection

In order to be allowed on the market, each car should pass a various number of safety regulations. The two main regulations that are influencing dummy development are the European and the United States regulations. In Europe, UNECE [4] regulations are applicable and regarding frontal impact, UNECE R 94 is used. Until 1998 Global Agreement, the United States were not part of UNECE and followed their own standards. For frontal impact FMVSS [5] 208 is applicable for all passenger cars sold in the United States.

In order to assess occupant protection during car crashes, these regulations perform impact tests with crash test dummies representing the car occupants. Injury criteria are defined in order to link the measurements performed by the dummies to occupant injury risk in the real world. However no injury criteria for the abdomen exists for the moment in regulations. Thorax injury criteria will be presented here as examples.

The frontal impact regulation in Europe consists in a a vehicle impacting a fixed deformable barrier (1 m width and 65 cm height placed 20 cm above the ground) at a 56 km h^{-1} speed with 40 % of the vehicle width overlap on the driver side. Two Hybrid III dummies seating in the front seats are used (UNECE R 94, see UNECE 2013).

The chest deflection and $(V \cdot C)_{\max}$ are used for the thorax. The chest deflection should be less than 50 mm and $(V \cdot C)_{\max}$ should not exceed 1 m s^{-1}. $(V \cdot C)_{\max}$ is computed as the maximum value of the product of compression and rate of chest deflection multiplied by 1.3 (scaling factor). The compression is the deflection divided by the sternum depth of 229 mm.

The United States regulation for frontal impact differs from the European regulation. The test

4. United Nations Economic Commission for Europe
5. Federal Motor Vehicle Safety Standard

consists in the vehicle impacting with full width a rigid barrier at $48\,\mathrm{km\,h^{-1}}$ (FMVSS 208, see NHTSA 2011). Two Hybrid III dummies are seated in the front seats. For the thorax the resultant acceleration should not exceed 60 g's and the chest deflection should not exceed 63 mm. The United States regulation also has a test for the 5th percentile female Hybrid III dummy that is similar to the test case of the European regulation but with a velocity of $40\,\mathrm{km\,h^{-1}}$.

1.1.3 NCAP and Euro NCAP assessment

The NCAP [6] was created by NHTSA in 1978 for cars on the United States market. NCAP goal is to keep on improving the safety of cars by giving rating to each car in the market. The frontal impact test protocol consists in the same test condition as the US [7] regulation with an increased speed of $56\,\mathrm{km\,h^{-1}}$ (NHTSA 2012). It uses the Hybrid III dummy in the driver position and 5th percentile female Hybrid III as passenger and the same injury criteria as the regulation are used with the same tolerance levels.

Euro NCAP [8] is an independent body created in 1997 (Hobbs and McDonough 1998) and backed by the European Commission, European Governments and motoring and consumers organisations. Euro NCAP has more stringent test conditions than the regulation and gives points to assess how good the protection of a body region is. When more than one injury criterion exist, the weakest performance is considered for points attribution. If the value of a criterion is below the higher performance limit, 4 points are given for the body region protection. If the value is above the lower performance limit, 0 points are given. If the value is in between, a linear interpolation is performed to calculate the number of points. Then a score is given to the body region according to Table 1.2. The Euro NCAP frontal impact tests has the same protocol than the European regulation tests, the impact velocity being higher at $64\,\mathrm{km\,h^{-1}}$ (Euro NCAP 2015d). Since 2015, a new test close to the US regulation has also been added with an impact speed of $50\,\mathrm{km\,h^{-1}}$ (Euro NCAP 2015c) with 5th percentile female Hybrid III dummies. This tests includes the assessment of submarining and decreases the car score in case of submarining. Submarining is assessed for driver and rear passenger by a 1 kN drop in any of the two iliac forces within 1 ms and video confirmation. Figure 1.4 shows the principle of the two tests. Table 1.3 shows the values of the $(V \cdot C)_{\max}$ criteria and chest deflection taken from Euro NCAP 2015b.

score	color	points
Good	green	4.000
Adequate	yellow	2.670 to 3.999
Marginal	orange	1.330 to 2.669
Weak	brown	0.001 to 1.329
Poor	red	0.000

Table 1.2 – Euro NCAP scores (Euro NCAP 2015b)

criterion	lower performance limit	higher performance limit	regulation values
deflection (mm)	42	22[a] / 18[b]	50[c] / 63[d]
$(V \cdot C)_{\max}$ ($\mathrm{m\,s^{-1}}$)	1	0.5	1[c]

Table 1.3 – Criteria and limit values for Euro NCAP tests (Euro NCAP 2015b)
[a]Offset-deformable barrier test [b]Full width rigid barrier test [c]European regulation [d]United States regulation

6. New Car Assessment Programme
7. United States
8. European New Car Assessment Programme

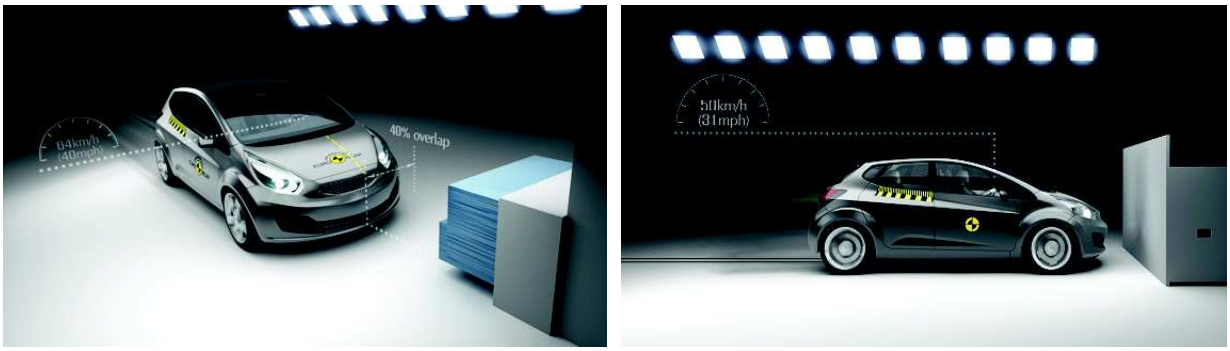

(a) Offset-deformable barrier test (b) Full width rigid barrier test

Figure 1.4 – Euro NCAP frontal tests (www.euroncap.com)

1.1.4 Future trends

The Hybrid III dummy used in the current regulation originates from the 1970's. It is planned to be replaced by the THOR dummy which has been developed by NHTSA since the 1990's. Figure 1.5 shows the two dummies.

NHTSA plans to introduce the THOR 50th percentile dummy in the NCAP program for full frontal tests and a new frontal oblique test condition (NHTSA 2015) for vehicles manufactured from 2019 onwards. On the other hand, in its 2020 roadmap (Euro NCAP 2015a), Euro NCAP describes the THOR mid-sized male dummy as an "enabler" for the "Mobile solution to offset front impact protection". This new test protocol is planned to be defined in 2018 and adopted in 2020. NHTSA is also elaborating a 5th percentile female version of the THOR dummy of which the abdomen would be one of the improved areas.

(a) Hybrid III (b) THOR

Figure 1.5 – Hybrid III and THOR dummies (www.humaneticsatd.com)

1.2 Abdomen response and injury mechanisms

1.2.1 Anatomy of the abdomen

Figure 1.6 shows the planes and directions of the human body. The abdomen is defined as the body region located between the diaphragm on the superior end and the pelvis on the inferior end. Figure 1.7 shows the global location of the abdomen in the human body. The abdomen consists of organs partly protected by skeletal structures and surrounded by muscles and skin. The abdomen can be divided in three parties:

— The upper abdomen or epigastric region is located between the diaphragm and the transpyloric plane
— The mid-abdomen or umbilical region is located between the transpyloric plane and the transtubercular plane
— The lower abdomen or hypograstric / pubic region is located between the transtubercular plane and the pelvis

The transtubercular plane is the transverse plane passing through the iliac tuberosities (see Figure 1.8a). This plane is close to the interspinous plane passing through the anterior superior iliac spines (Figure 1.8b), which can also be used to define the limit mid / lower abdomen. The transpyloric plane is a transverse plane locate halfway between the superior end of sternum (jugular notch) and the inferior end of the pelvis (superior aspect of the pubic symphysis, Figure 1.8b). The location of these planes is reported on Figure 1.7.

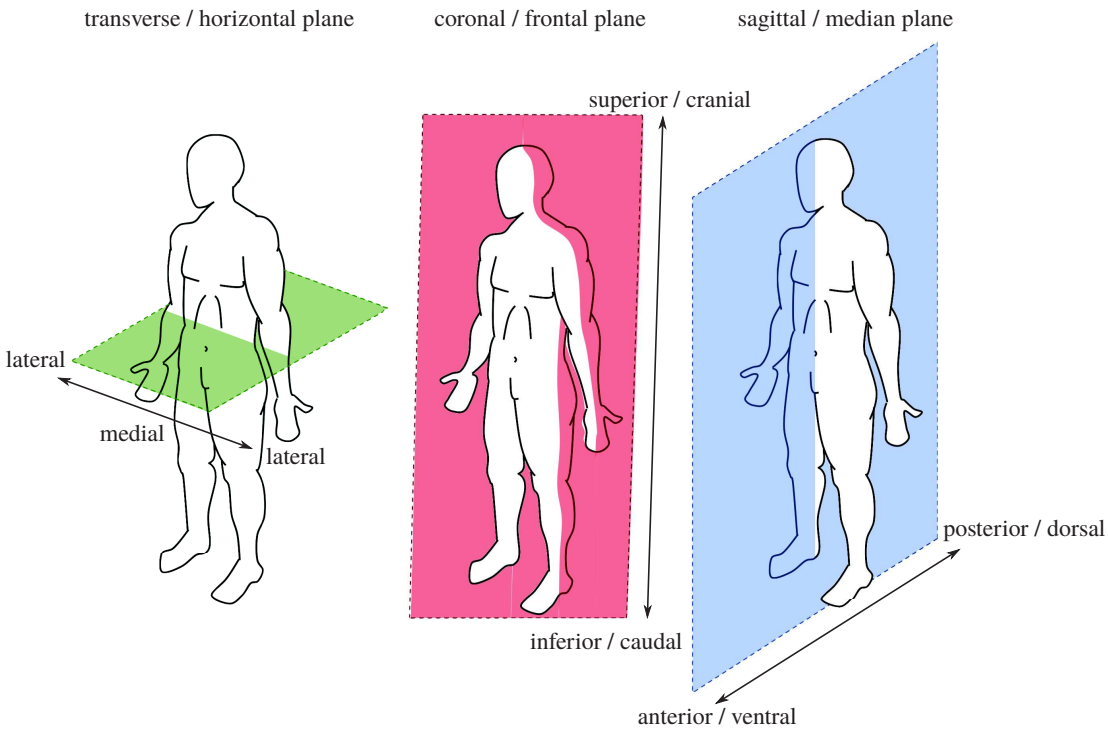

Figure 1.6 – Human planes and body directions (`commons.wikimedia.org`)

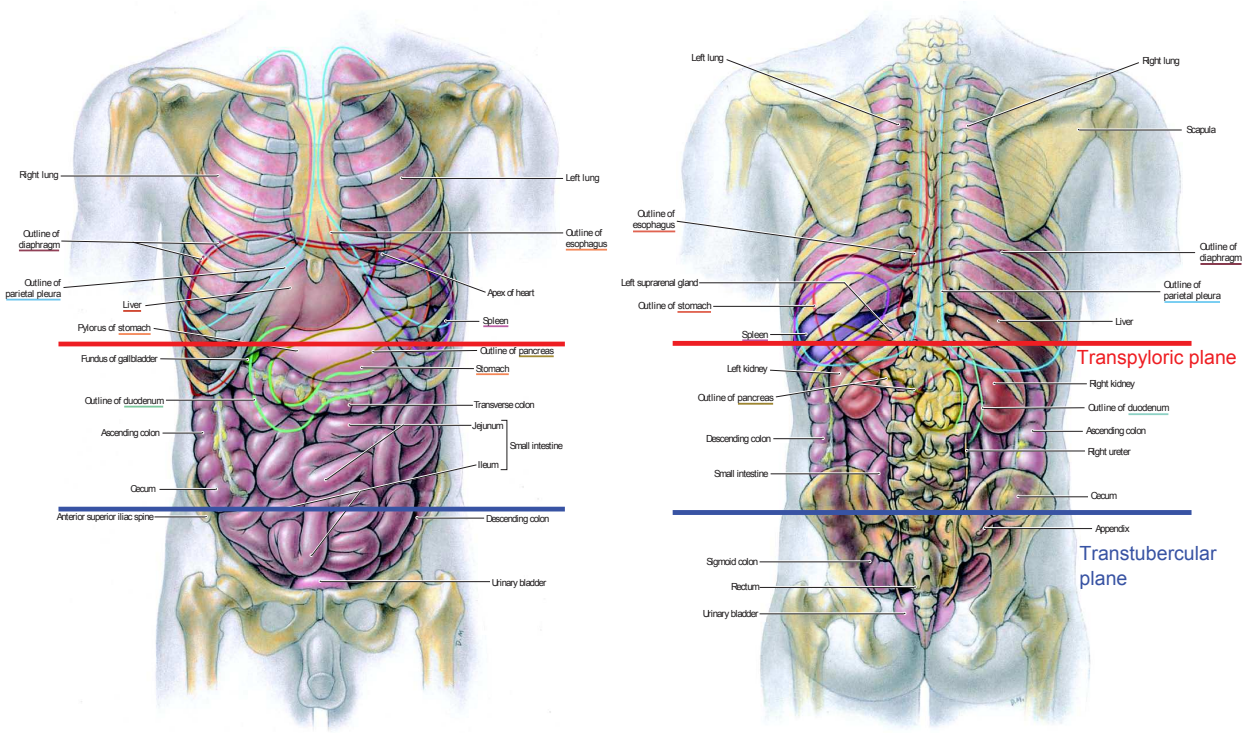

(a) Anterior view (b) Posterior view

Figure 1.7 – Global view of the abdomen (Agur and Dalley 2013)

1.2.1.1 Skeletal system

The abdomen is in relation with three main bony structures. At the inferior end, the pelvis protects the urinary system and includes part of the small intestine. The spine is located at the posterior side of the abdomen. The thoracic and lumbar vertebrae are located in the abdomen zone as well as the sacrum. The sacrum is linked to the hip bones, altogether making the pelvis. Figure 1.8 shows the pelvis, an overview of the spine and the details of a vertebra. At last, the ribcage protects the organs of the upper abdomen.

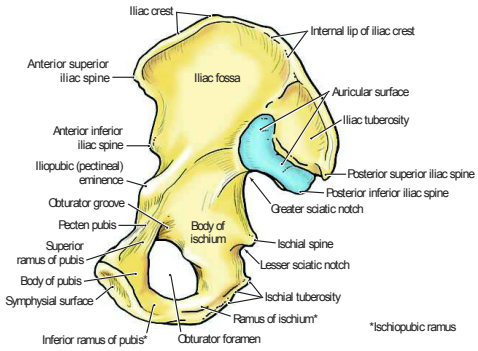

(a) Medial view

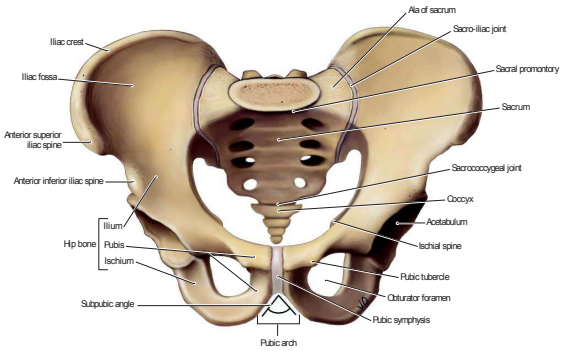

(b) Anterior view

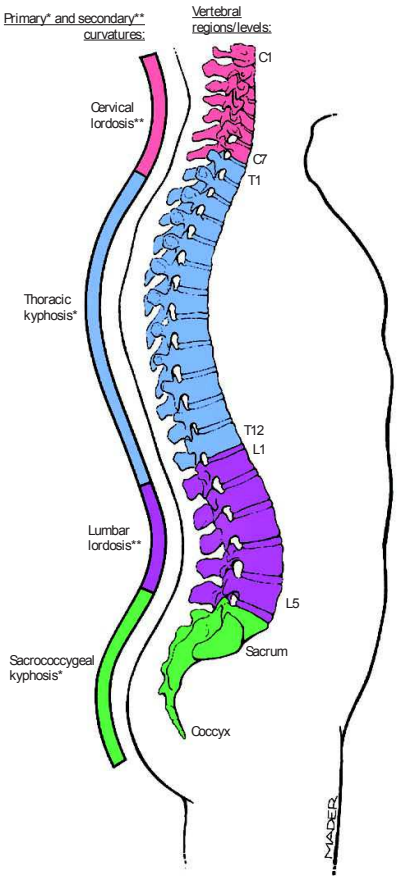

(c) Lateral view of the spine

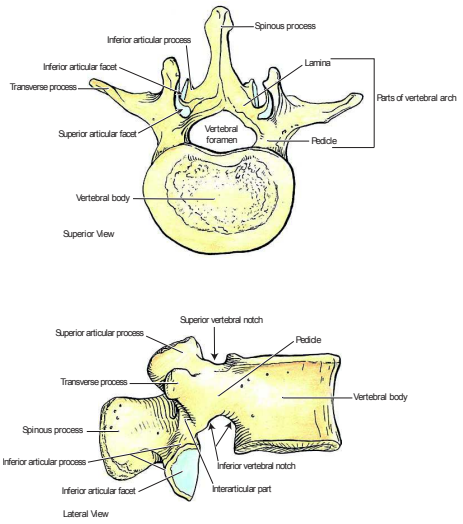

(d) Superior and lateral views of a vertebra

Figure 1.8 – Views of the spine (Agur and Dalley 2013)

1.2.1.2 Muscular system

The organs of the abdomen are surrounded by muscles that keep them compressed in the abdominal cavity. Main muscles include the diaphragm, the rectus abdominis, the external oblique, the internal oblique and the tranversus abdominis. The presence of subcutaneous fat is also important regarding the impact response of the abdomen. The diaphragm is a dome-shaped structure attached to the abdominal wall, the sternum, the ribs and the vertebrae T12 [9], L1 [10] and L2 [11]. The rectus abdominis is a paired muscle located on the anterior side of the abdominal wall. It goes from the pubis to the sternum and costal cartilages. The external oblique is located on the anterior side of the abdominal wall and is linked to the lower ribs and to the iliac crest. The internal oblique lies below the external

9. 12th thoracic vertebra
10. 1st lumbar vertebra
11. 2nd lumbar vertebra

oblique, perpendicular to it. It goes from the costal cartilage to the iliac crest. The tranversus abdominis is located below the internal oblique and goes from the sternum and rib cartilage to the pubis and the iliac crest. Figure 1.9 shows the different layers of muscles in the abdomen region.

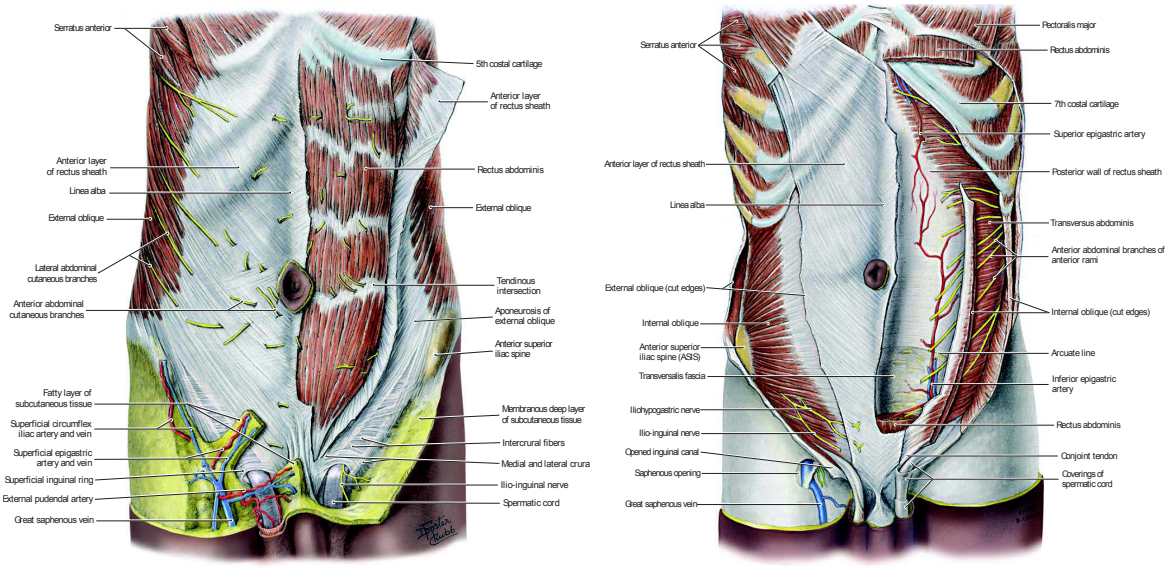

(a) Superficial dissection (b) Deep dissection

Figure 1.9 – Anterior views of abdominal muscles (Agur and Dalley 2013)

1.2.1.3 Organs

The organs of the abdomen participate to different functions essential to the human body. The liver, gallbladder and pancreas are part of the digestive system as well as the organs that constitute the digestive tract: the stomach, small intestine and the colon (also named large intestine). The digestion takes place first in the stomach, then in the small intestine and at last in the large intestine. The urinary system is composed of the kidneys, the ureters and the urinary bladder. The spleen is an organ that plays a role in the immune system and for blood cells management. Among them, the liver, the pancreas and the two kidneys (together) are vital organs for which a major injury could lead to death. AIS 6 (maximum) is only defined for the liver, compared to AIS 5 (critical) for the pancreas and the kidneys (AAAM 2005).

The organs can also be divided into solid and hollow organs. The solid organs are the liver, the spleen, the kidneys and the pancreas. These organs are located in the upper abdomen and are partially covered by the rib cage. Figures 1.10a to 1.10d show the liver, the kidneys and the spleen. The hollow organs are the gallbladder, the stomach, the small intestine, the colon, the ureters ans the urinary bladder. They are located in the mid and lower abdomen.

The organs are attached by various ligaments and membrane, among them are the peritoneum and the mesentery. The peritoneum covers the most of the abdominal organs and connects them to the abdominal wall. The peritoneal cavity consists of two main region, the greater sac and the lesser sac. The mesentery goes from the posterior wall of the peritoneal cavity and attaches to the intestinal tract. It links the different structures of the small intestine to the peritoneum. Figures 1.10e and 1.10f show the hollow organs and membranes of the abdomen.

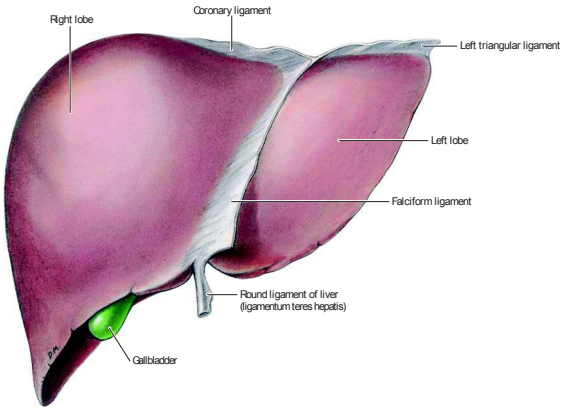

(a) Anterior view of the liver

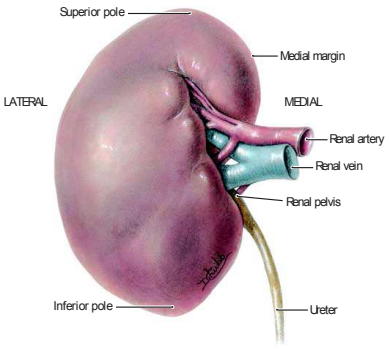

(b) Anterior view of the kidney

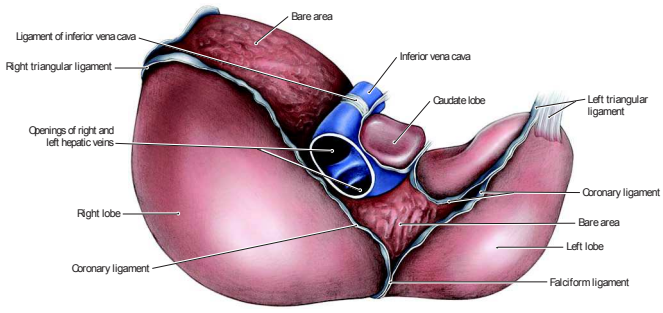

(c) Superior view of the liver

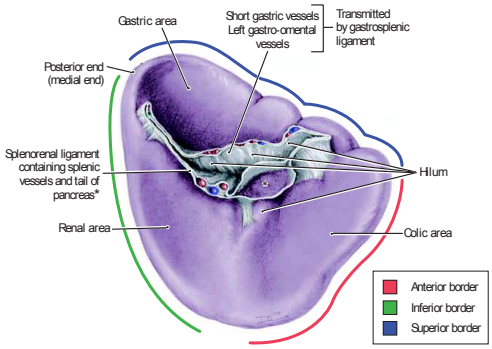

(d) Inferomedial view of the spleen

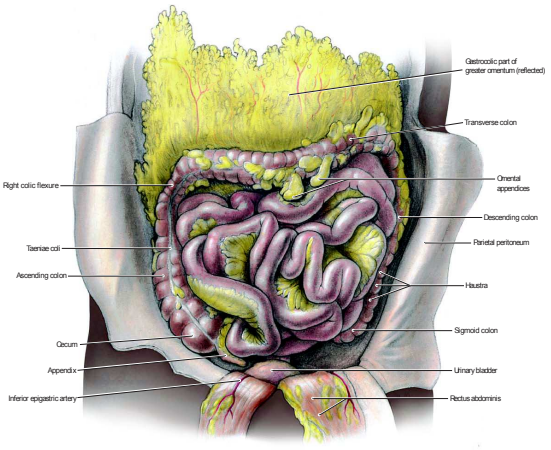

(e) Anterior view of the small intestine and colon

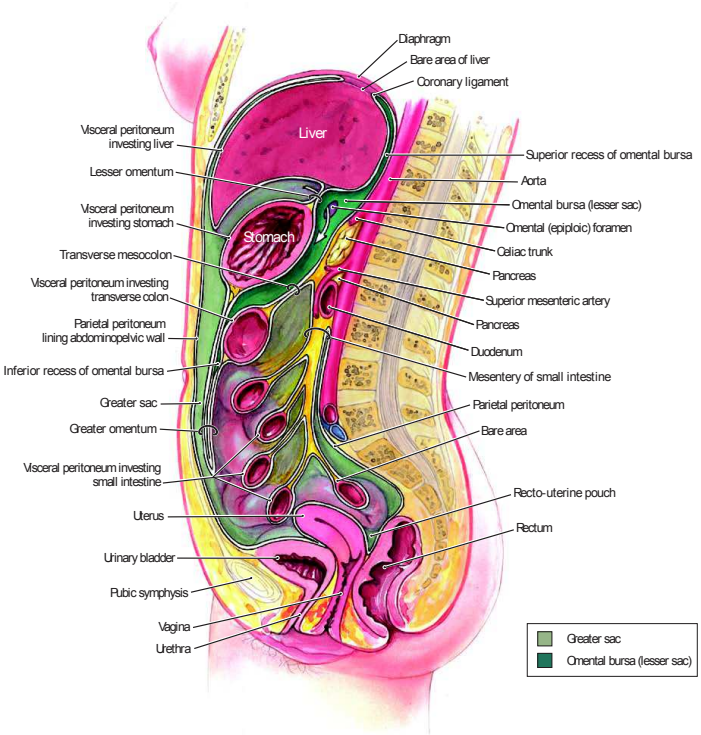

(f) Median section of the abdomen showing mesentery and peritoneum

Figure 1.10 – Solid and hollow organs and membranes of the abdomen (Agur and Dalley 2013)

1.2.2 Accidentology of the abdomen

In order to classify the injuries sustained by car occupants after a crash in a standardised manner, the AIS scale has been developed (AAAM 2005). This system allows to classify any injury by mentioning the body region, the type of anatomical structure, the specific anatomical structure, the level and the AIS score itself. The AIS score describes the severity of the injury. Six levels of increasing severity are defined as mentioned in Table 1.4. The MAIS [12] is the maximum AIS value that a subject sustained to any body part. In order to indicate all the injuries with a minimum AIS of 3 (for instance), the term AIS 3+ is used.

AIS score	description
1	minor
2	moderate
3	serious
4	severe
5	critical
6	maximum

Table 1.4 – Injury severity score (AAAM 2005)

Over the years, seatbelt use and airbag availability modified the sources of injury to the abdomen. This trend has been illustrated for thorax injuries in Kent et al. 2004 and the general statements are valid for the abdomen region. While seatbelt use and airbag availability grew, the proportion of injuries created by the steering wheel decreased whereas the proportion of those created by the seatbelt and the airbag grew. At the end of the 1990's, the seatbelt overtook the steering wheel as main cause of thoracic injuries (Figure 1.11). However results from Kent et al. 2003 clearly show that seatbelt and airbag reduce the probability of injuries (all body regions considered) in frontal crash (Figure 1.12). The principal source of injury vary depending on which organ is considered. Elhagediab and Rouhana 1998 reported that for the abdomen the steering wheel is the main source of injuries for the liver and the spleen but that the seatbelt is the main source of injuries for the digestive system (Table 1.5). Overall 69 % of abdominal injuries are due to the steering wheel and 17 % to the seatbelt. These data represent accidents from 1988 to 1994 so the recent evolution of restraint systems is not included. Klinich et al. 2010 reported more balanced proportions with 50 % AIS 3+ injuries created by the steering wheel and 30 % by the seatbelt for 1998–2008 accidents. They also reported the decrease of abdominal injuries with more recent vehicle model year. The most recent study, Shin et al. 2015 reported that the seatbelt overtook the steering wheel as primary source of abdomen injuries with 64 % of injuries due to the seatbelt and 22 % due to the steering wheel based on 2009–2012 data. This proves that the trend predicted for the thorax in Kent et al. 2004 is also effective for the abdominal region.

	LIVER	SPLEEN	ARTERIES	DIGESTIVE	KIDNEYS	RESPIRATORY	UROGENITAL	TOTAL
BELT	1.63%	2.34%	1.54%	9.62%	1.26%	0.56%	0.00%	**16.95%**
SW	34.31%	13.72%	9.07%	6.68%	0.76%	2.69%	1.49%	**68.72%**
BAG	0.00%	0.13%	0.00%	0.00%	0.00%	0.00%	0.00%	**0.13%**
INTERIOR	3.26%	6.89%	1.37%	0.84%	0.14%	0.77%	0.93%	**14.19%**
TOTAL	**39.20%**	**23.08%**	**11.98%**	**17.13%**	**2.17%**	**4.02%**	**2.41%**	**100.00%**

Table 1.5 – Injury sources for abdominal organs (Elhagediab and Rouhana 1998)
SW: Steering Wheel

Lamielle et al. 2006 described that solid organs were more injured than hollow organs but with close proportions (46 % and 43 %). It has also been demonstrated that the use of a restraint system was shifting the injuries from solid organs to hollow organs for front occupants (Table 1.7). Modern

12. Maximum AIS

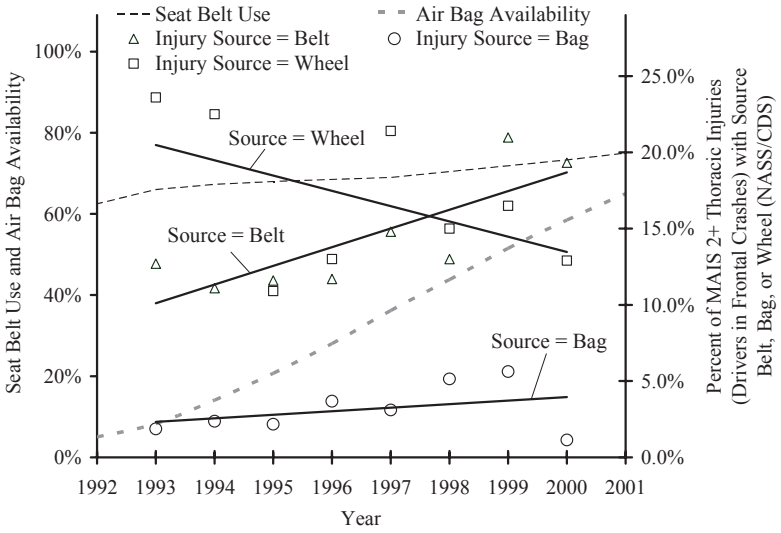

Figure 1.11 – Source of thoracic injuries to drivers in frontal crash compared to seatbelt use and airbag availability trends (Kent et al. 2004)

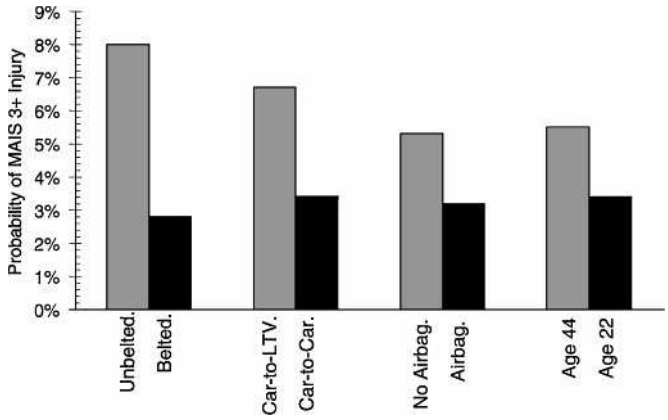

Figure 1.12 – Relative injury probability in frontal crash influenced by seatbelt and airbag use (Kent et al. 2003)

cars equipped with retractable seatbelts, pretensioners and airbags have an injury proportion of 62 % for the hollow organs compared to 38 % for solid organs.

Liver has been described as the most injured abdominal organ in Elhagediab and Rouhana 1998 followed by spleen and the digestive system, base on US data (Table 1.5). Frampton et al. 2012 described similar results but Lamielle et al. 2006 described the spleen as the most injured organ followed by the liver and the jejunum, part of the digestive system based on French data (Table 1.6). The differences in results between these two studies is explained in Lamielle et al. 2006 by the fact that there is more unbelted occupants in the US compared to France. Yoganandan et al. 2000 described the spleen (31 %) and the liver (30 %) as the most injured organs followed by the kidneys (19 %) and the digestive system (11 %). These data included frontal and side impact which explains the presence of kidneys injuries. These results highlight that there is a need to pay particular attention to the hollow organs protection with today's car, and that those injuries are be mainly created by the seatbelt.

	Organs	AIS 3+ Injuries
Solid organs	Liver	101
	Spleen	141
	Kidneys	21
	Pancreas	17
Hollow organs	Duodenum	11
	Jejunum	102
	Colon	47
	Mesentery	82
	Stomach	6
	Bladder	14
	Others	72
	Total solid	280
	Total hollow	262
	Total	634

Table 1.6 – Distribution of abdominal organs injuries (Lamielle et al. 2006)

	%hollow	%solid	%hollow	% solid
Unbelted	23%	77%	23%	77%
SB	63%	38%	58%	42%
RB	55%	45%		
RB+P	50%	50%		
RB+P+AB	62%	38%		

Table 1.7 – Hollow and solid organs injuries depending on the restrain system for front occupants (Lamielle et al. 2006)
SB: Three point static belt
RB: Three point belt plus retractor
RB+P: Three point belt plus retractor and pretensioner
RB+P+AB: Three point belt plus retractor, pretensioner and frontal airbag

1.2.3 Abdomen mechanical response

The mechanical response of the human abdomen can be assessed by different means, either by volunteer tests, animal tests or tests on PMHS. It has been chosen here to review frontal impact PMHS tests given the fact that volunteer test can only give information on very low severity loading and that animal testing can not be considered as a way of assessing adult human response due to the anthropometry mismatch. Two main categories of test have been designed to reproduce the abdomen contact with the steering wheel or the abdomen loading by a seatbelt.

1.2.3.1 Impactor tests

In order to represent the contact of the abdomen with the steering wheel of a car, many studies used an impactor protocol. Figure 1.13 shows the test set-up of the considered studies and Figure 1.14 presents the responses of the subjects in the force-penetration diagram.

The first impactor study on PMHS was done by Cavanaugh et al. 1986, where 12 subjects were tested. The subjects were impacted at the level of the L3 [13] vertebra by a 25 mm diameter rigid bar, their back being unrestrained. The L3 level was chosen because it corresponds to an impact at mid-abdomen level (in terms of height) and prevents interaction with the lower ribcage. The nominal mass assigned to the impactor was either 32 kg or 64 kg. The nominal impact velocity varied from $5\,\mathrm{m\,s^{-1}}$ to $13\,\mathrm{m\,s^{-1}}$.

Impactor test were also conducted in Hardy et al. 2001 with a free back condition. Both the mid-

13. 3rd lumbar vertebra

abdomen (L3 level) and upper abdomen (T11 [14] level) were impacted by a 25 mm diameter impactor having a mass of 48 kg. The subjects were impacted at 6 m s^{-1} (3 subjects at the mid-abdomen level and 2 subjects at the upper abdomen level) and 9 m s^{-1} (3 subjects at the mid-abdomen level and 1 subject at the upper abdomen level).

Shaw et al. 2004 used a steering wheel-like impactor on four subjects. The impactor was inclined at 45° and the subject back was fixed. The impactor diameter was 25 mm and it had a mass of 64 kg. The impact velocity was of 4 m s^{-1}. The impactor was at the level of the T12 vertebra in order to impact the upper abdomen. The impactor penetration in the abdomen was limited to 30 % of the abdomen depth for three subjects and to 50 % for one subject.

(a) Cavanaugh et al. 1986 (picture from Lee and Yang 2001)

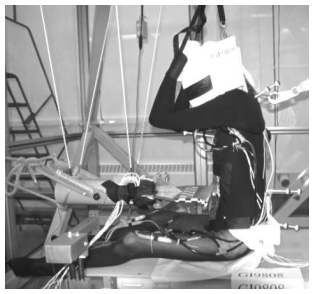

(b) Hardy et al. 2001 mid-abdomen

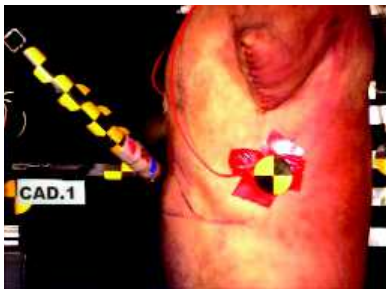

(c) Shaw et al. 2004

Figure 1.13 – Impactor test set-ups from the considered studies

14. 11th thoracic vertebra

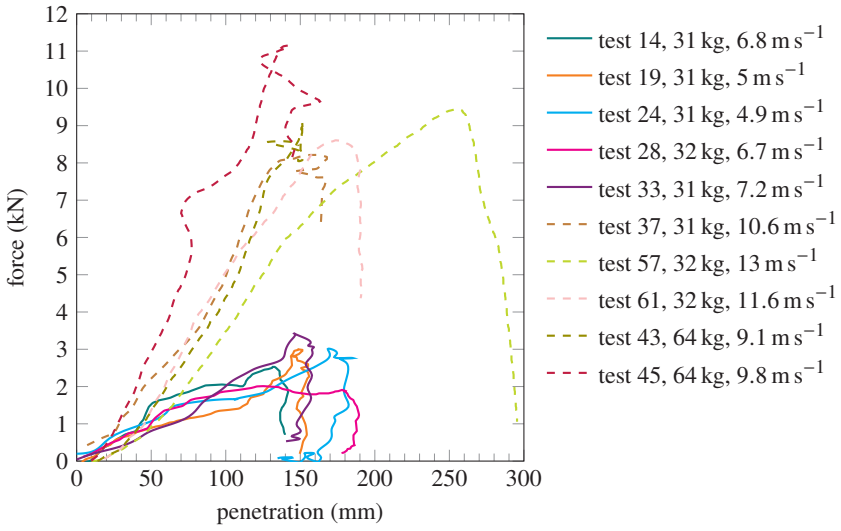

(a) Cavanaugh et al. 1986

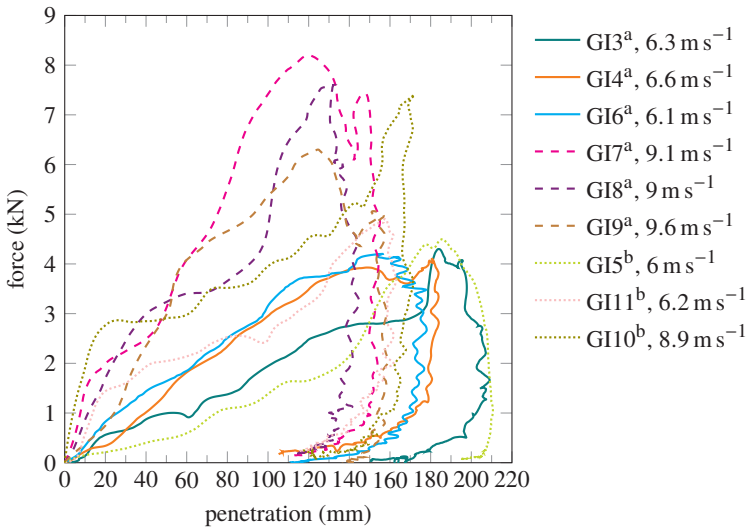

(b) Hardy et al. 2001 (free back condition)

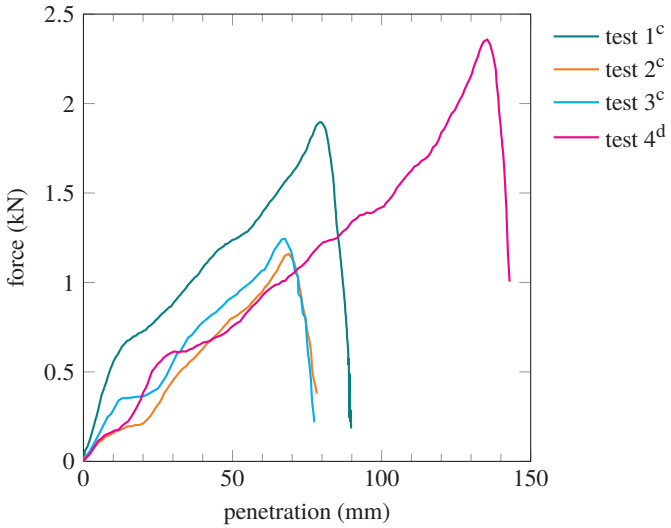

(c) Shaw et al. 2004

Figure 1.14 – Subjects responses under impactor tests for the considered studies

[a]impact at mid-abdomen level

[b]impact at upper abdomen level

[c]Penetration limited to 30 % of torso depth

[d]Penetration limited to 50 % of torso depth

1.2.3.2 Seatbelt tests

In addition to impactor tests, test protocols have also been developed in order to study the behaviour of the abdomen under compression by a seatbelt. Figure 1.15 shows the test set-up of the considered studies and Figure 1.16 presents the responses of the subjects in the force-penetration diagram.

Seatbelt test were performed in Hardy et al. 2001 on three subjects. These tests are the only free back reported tests. The seatbelt was driven by a pneumatic ram with adjusted pressure to produce the desired loading velocity. A peak velocity of $3\,\mathrm{m\,s^{-1}}$ was imposed and a haversine speed-time input condition was obtained. The belt was placed on the mid-abdomen.

In Trosseille et al. 2002, six subjects were tested under a seatbelt loading on the mid-abdomen, the back of the subject being restrained. Two configurations were performed with custom-made pyrotechnic devices:

— *configuration 1* with one pretensioner on one side having 28 kJ of pyrotechnic input and presence of a load limiter of which the limiting force value was not mentioned by the authors.
— *configuration 2* with one pretensioner one each side having 3.2 kJ of pyrotechnic input each.

Three seatbelt retracting conditions were performed in Foster et al. 2006. Two conditions were with one pretensioner retracting the seatbelt (called B and C, the B conditions being of higher energy) and one condition was with two B pretensioners in parallel (called A). Four subjects were tested under the A condition, three under the B condition and one under the C condition (twice). The region loaded was the mid-abdomen.

The study Lamielle et al. 2008 targeted two different velocity ranges aiming to reproduce the conditions of either submarining (retraction velocity around $4\,\mathrm{m\,s^{-1}}$ and penetration around 100 mm) and OOP [15] loading (retraction velocity around $8\,\mathrm{m\,s^{-1}}$ and penetration around 60 mm). The submarining-like series was named MHA and the OOP-like series was named PRT. Eight PMHS were tested, allowing 4 tests of each configuration. The mid-abdomen was loaded either by an hydraulic piston (MHA series) or by pretensioners (PRT series), the subject's back being fixed. In the MHA series, the retraction velocity and the maximum belt displacement were imposed as reported in Table 1.8 with targets in terms of penetration velocity and abdomen compression.

(a) Hardy et al. 2001 (b) Trosseille et al. 2002 (with THOR dummy as demonstrator) (c) Foster et al. 2006 (d) Lamielle et al. 2008

Figure 1.15 – Seatbelt test set-ups from the considered studies

test	penetration velocity ($\mathrm{m\,s^{-1}}$)	penetration (percentage of abdomen depth)
MHA111	4	30
MHA115	5	40
MHA151	4	40
MHA155	5	30

Table 1.8 – Input parameters from Lamielle et al. 2008 MHA tests, according to Lamielle 2008

15. Out Of Position

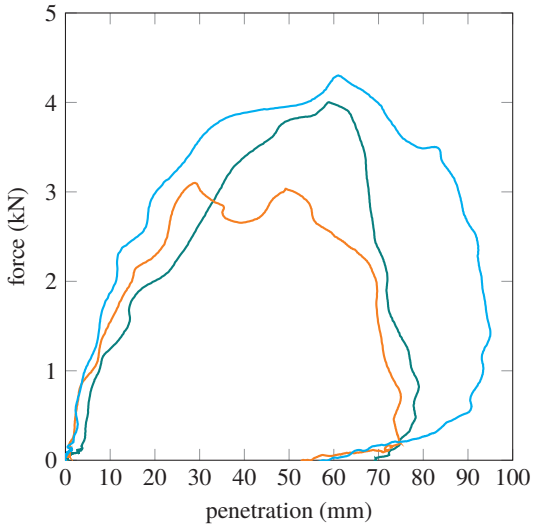

(a) Hardy et al. 2001 responses

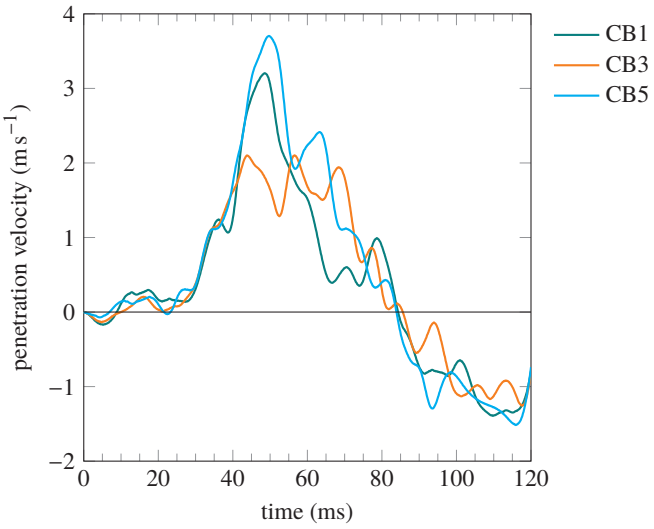

(b) Hardy et al. 2001 input conditions

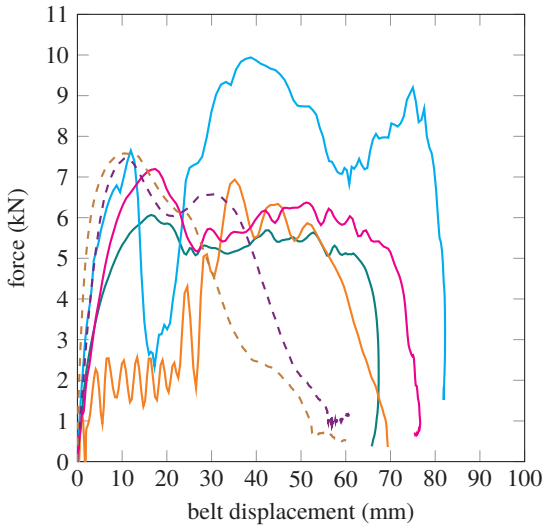

(c) Trosseille et al. 2002 responses

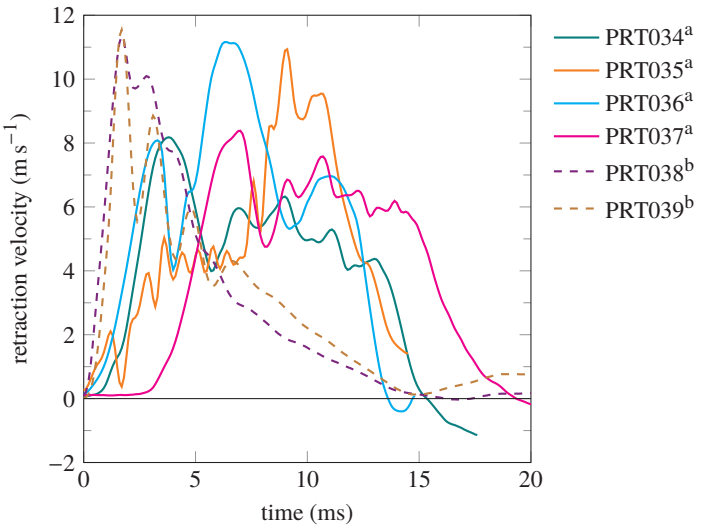

(d) Trosseille et al. 2002 input conditions

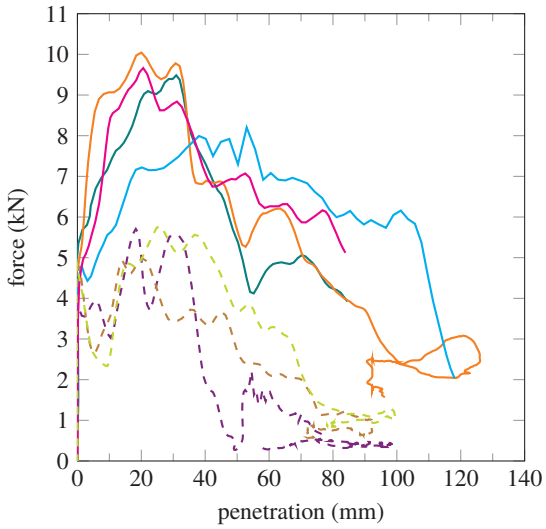

(e) Foster et al. 2006 responses

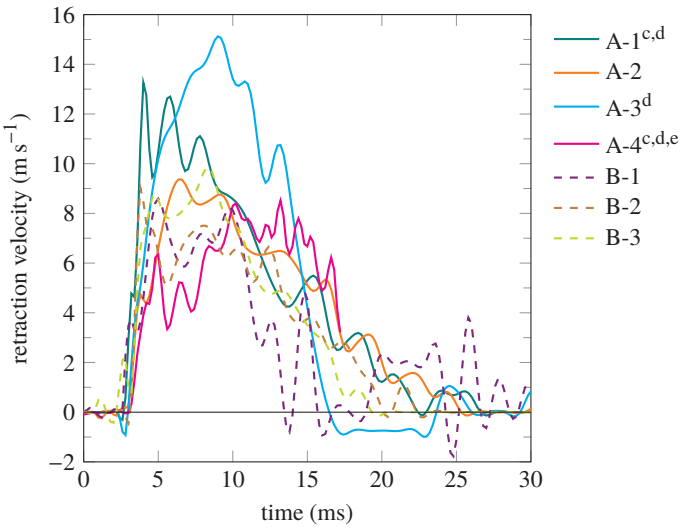

(f) Foster et al. 2006 input conditions

Figure 1.16 – Subjects responses under seatbelt tests for the considered studies

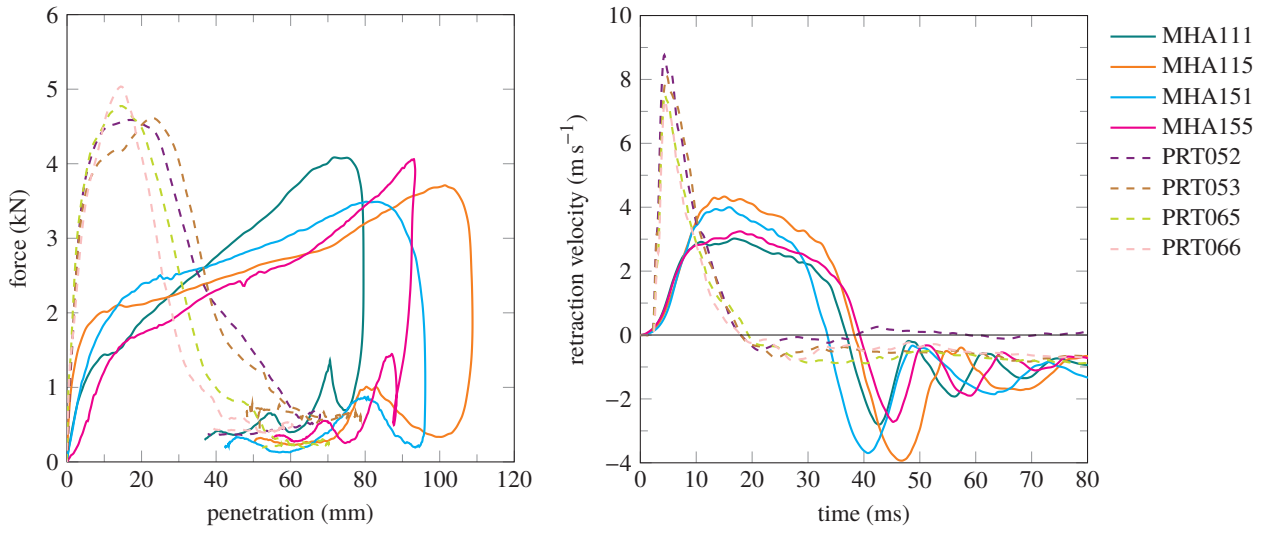

(g) Lamielle et al. 2008 responses

(h) Lamielle et al. 2008 input conditions

Figure 1.16 – Subjects responses under seatbelt tests for the considered studies (continued)

[a] *configuration 1*

[b] *configuration 2*

[c] Penetration values from laser measurement instead of video measurement

[d] Penetration could not be measured until the end of the test

[e] Retraction velocity measurement not available, penetration velocity used instead

For the impactor condition, the results from Hardy et al. 2001 match those from Cavanaugh et al. 1986 in terms of abdomen stiffness for low and high speed impact, although the impactor mass is different. A rate-sensitivity of the abdomen has been highlighted with a stiffer response for a higher impact velocity in both studies.

For seatbelt tests, Trosseille et al. 2002 reported that although the input conditions were believed to be significantly different, no difference was seen in the abdomen response. Differences were however reported in the injury statements. The differences in abdomen loading induces a difference in mechanical response. When the abdomen is loaded with a pretensioner the response shows a high initial force peak at very low penetration which means that the abdomen has very stiff behaviour compared to a loading with a piston or a ram. The rate sensitivity has however also been highlighted, a higher retraction velocity leading to a higher peak force in each case.

A variability of the human response appears from the PMHS test data due to the variety of anthropometric dimensions of the human subjects which leads to the need of developing harmonised response corridors.

1.2.3.3 Biofidelity corridors

The need to provide harmonised references for the evaluation of crash test dummies of numerical human models lead to the development of biofidelity corridors based on PMHS tests. Corridors represent a domain on a graph (usually force / penetration for moment / angle) in which a dummy or model response curve should fit in order to be assessed biofidelic. The borders of the corridor could be either standard deviation values from the average PMHS response or an envelope including all PMHS responses.

Recent harmonised corridors have been developed in Lebarbé et al. 2015. Based on PMHS tests

from the literature mean response data and boundaries are provided. For force and penetration versus time targets, standard deviations values are defined boundaries. For force versus penetration targets, the boundaries are computed as standard deviation ellipses according to the method described in Shaw et al. 2006. Figure 1.17 shows the corridors from Lebarbé et al. 2015.

For the impactor loading case, data from Cavanaugh et al. 1986 have been selected. A first corridor was generated for subjects impacted with a 32 kg mass and a low velocity (average 6.1 m s^{-1}). A second corridor was generated for subjects impacted with either a 32 kg or 64 kg mass and a high velocity (average 10.8 m s^{-1}). The PMHS responses were normalised with the technique described in Mertz 1984 based on subject body mass and abdomen depth before generating the corridors.

For the seatbelt case, the MHA test series from Lamielle et al. 2008 have been used to generate the corridor. This series was chosen because it had been originally designed to represent a submarining phenomenon in terms of abdominal loading. No normalisation was applied and the existing normalisation methods were described as adapted for blunt impacts with an impactor having significant mass but not for belt loadings.

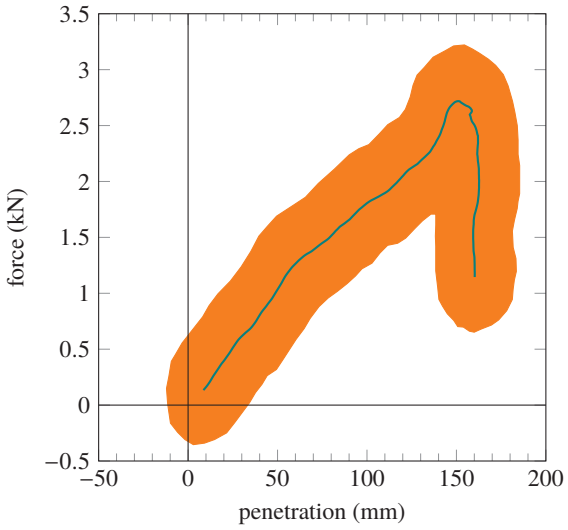

(a) Cavanaugh et al. 1986 low speed condition

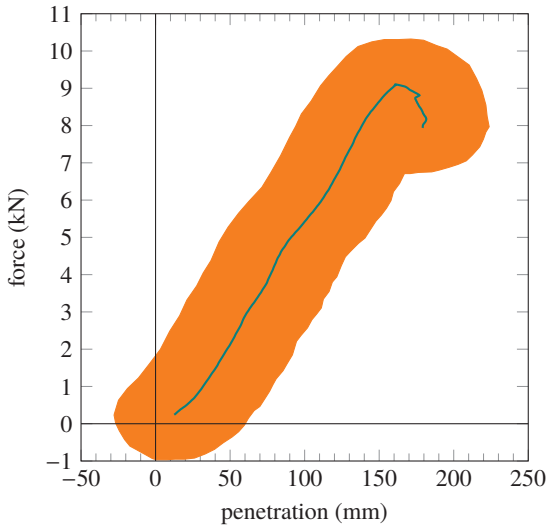

(b) Cavanaugh et al. 1986 high speed condition

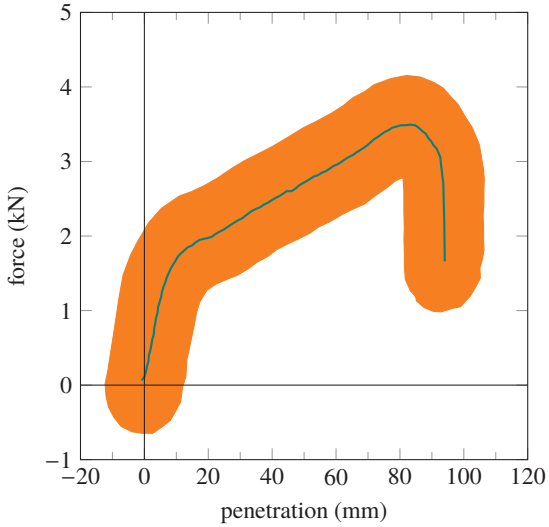

(c) Lamielle et al. 2008 MHA condition

Figure 1.17 – Corridors from Lebarbé et al. 2015

1.2.4 Abdomen injury mechanisms

1.2.4.1 Injury types

The injury types to the abdomen were reported by Lee and Yang 2002 to be mainly contusions (43 % of the total injuries), lacerations (28 %) and abrasions (13 %). When looking at serious to critical, it has however been found that only lacerations were significantly AIS 3+ injuries, along with ruptures and avulsions. Shin et al. 2015 reported that 58 % of the abdomen injuries are contusions and 23 % are lacerations. Contusions were reported to be caused by the steering wheel whereas lacerations were caused by both steering wheel and seatbelt.

Figure 1.18 shows results from Bansal et al. 2009 classifying abdomen injuries types and severity. It appears that AIS 5+ injuries are only liver and spleen lacerations.

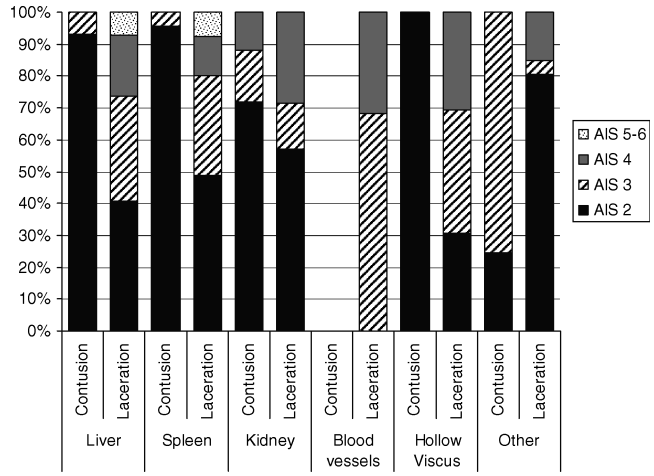

Figure 1.18 – Abdominal injury description and severity (Bansal et al. 2009)
Hollow Viscous includes colon, small intestine, uterus, bladder and stomach
Other includes mesentery, adrenal gland, pancreas, uro-genital organs, skin, omentum and retroperitoneal hemorrhage
Rupture and abdominal organ destruction were included in the laceration category

Regarding PMHS tests, tears and lacerations of liver have been reported in Hardy et al. 2001 impactor tests along with spleen and cecum tears. No other impactor test studies reported injuries. For seatbelt tests, Trosseille et al. 2002 reported a spleen rupture, a mesentery tear and an omentum tear. Foster et al. 2006 reported liver lacerations and tears, lobe transections and disruptions as well as spleen tears. A detailed injury statement has been provided in Lamielle et al. 2008: liver, spleen, pancreas lacerations and tears, mesentery contusions, lacerations and abrasions, colon, jejunum-ileum, duodenum contusions and lacerations. A kidney injury has also been reported.

Injury statements were also reported to be dependent on the subject perfusion method. For instance no organ injuries were reported in Cavanaugh et al. 1986, due to the absence of local vasculature perfusion according to the authors. A perfusion at the organ level has been performed in Lamielle et al. 2008 which can explain the detailled injury statement provided. Detailed injury statements and perfusion conditions can be found in Appendix B.

The only studies presenting a consistent injury statement across a majority of subjects were Hardy et al. 2001 impactor conditions along with Foster et al. 2006 A condition and Lamielle et al. 2008. Tables 1.9, 1.10 and 1.11 show simplified injury statements for those conditions.

region	impact velocity ($m\,s^{-1}$)	liver AIS (injured subjects / number of subjects)
mid-abdomen	6	4 (3 / 3)
	9	4 or 5 (2 / 3)
upper abdomen	6	3 or 4 (2 / 2)
	9	4 or 5 (1 / 1)

Table 1.9 – Simplified injury statement from Hardy et al. 2001 impactor tests, with mention of injuries occurrence

condition	liver AIS (injured subjects / number of subjects)
A	3 (3 / 4)
B	/ (/)

Table 1.10 – Simplified injury statement from Foster et al. 2006, with mention of injury occurrence

con-dition	mesentery AIS (injured subjects / number of subjects)	colon AIS (injured subjects / number of subjects)	jejunum-ileum AIS (injured subjects / number of subjects)
MHA	/	/	2 (3 / 4)
PRT	2 (3 / 4)	3 (3 / 4)	2 (4 / 4)

Table 1.11 – Simplified injury statement from Lamielle et al. 2008, with mention of injury occurrence

1.2.4.2 Abdomen loading types

In a car accident, contusions, lacerations and abrasions can be mostly due to contact between car elements (steering wheel, dashboard) or compression by the seatbelt but ruptures and avulsions can also be due to motion of the organs inside the abdominal cavity as a result of deceleration.

If a car occupant is properly restrained, the seatbelt lies on the pelvic bone which prevents the abdomen from being loaded during the crash. However, a misplacement of the seatbelt, on top of the abdomen instead of on top of pelvis can lead to direct abdomen compression during the crash, especially with the use of seatbelt pretensioners. An other phenomenon leading to direct abdomen loading by the seatbelt is when the seatbelt, although originally positioned on the pelvis, slides over the pelvis to load the abdomen. This phenomenon is called submarining and can happen particularly because of a slouched position of the occupant. Submarining happens when the force acting on the pelvis are not in equilibrium and produce pelvis rotation. These two phenomenons are difficult to identify in the accidentology due to the lack of data on what is happening during a crash. However, they were successfully replicated in sled testing on PMHS. The most recent studies on submarining with PMHS subjects are Luet et al. 2012 and Uriot et al. 2015b.

1.2.4.3 Injury criteria

An injury criteria for blunt abdominal trauma is a mathematical relationship which links the occurrences of an injury observed during tests and physical parameters of those tests. A logistic regression is used to generate risk curves linking the value of the physical parameters and the probability of injury of a specified severity.

Many variables have been considered to be injury predictors. Abdomen compression (C), loading velocity (V), force exerted on the abdomen (F) and intra-abdominal pressure (P) were the most used. Combinations of those parameters have been proposed as injury criteria for the abdomen. Rouhana et al. 1985 proposed $V_{\max} \cdot C_{\max}$ as criterion and called it the Abdominal Injury Criterion. Viano and Lau 1985 proposed $(V \cdot C)_{\max}$, called the Viscous Criterion. Injuries at high compression and low loading velocity have been described in Lau and Viano 1986 as crushing injuries, those with moderate compression and velocity as viscous injuries and those with high velocity and low compression as blast injuries. Kent et al. 2008 conducted a study comparing all the existing criteria to date. The test condition was belt loading on supine porcine subjects. For single parameters,

maximum values of belt force and penetration were reported good injury predictors whereas the velocity was not. Regarding multi-parameters criteria, $V_{\max} \cdot C_{\max}$ and $(V \cdot C)_{\max}$ had similar abilities to predict injuries but newly proposed criteria, $\left(\dot{F} \cdot C\right)_{\max}$ and $F_{\max} \cdot C_{\max}$ had better results, the latter being the best predictor. Kent et al. 2008 also stated that $V_{\max} \cdot C_{\max}$ and $(V \cdot C)_{\max}$ were predicting less accurately injuries than the compression alone, questioning the added value of the loading velocity in the injury criteria, high loading velocity being well correlated with high compression in most studies.

Regarding pressure as an injury criteria, Sparks et al. 2007 investigated pressure-based predictors based on isolated human liver drop tests. In Kremer et al. 2011 where those data have been reprocessed, the best predictors were found to be $\dot{P}_{\max}$, $V_{\max} \cdot C_{\max}$ and $P_{\max}$. Kremer et al. 2011 also performed oblique impact PMHS tests with pressure sensors in the hepatic veins of the liver. $\dot{P}_{\max} \cdot P_{\max}$ and $\dot{P}_{\max}$ were reported to be the best predictors. Based on accident reconstruction with child dummies, Beillas et al. 2012 also reported $P_{\max}$, $\dot{P}_{\max}$ and $\dot{P}_{\max} \cdot P_{\max}$ as satisfactory injury predictors. $\dot{P}_{\max} \cdot P_{\max}$ had been previously proposed in Johannsen et al. 2007.

1.3 Tools for the evaluation of abdomen protection

1.3.1 Computer models

In order to be able to estimate the human body behaviour in case of a car crash, computer models of the human body have been developed. The accuracy of these models to represent the human body allows to get a better understanding of how the human body would behave than a physical test with a dummy. The improvements of computing capabilities and of medical imaging allowed to generate finite element models with more and more detailed organ representation. This bring the advantage to be able to analyse the loading of the internal organs of the body and to analyse the values of engineering parameters such as stresses and strains for local areas of the body. This would allow a precise injury prediction.

In order for these models to be used with the aim of injury prediction, their response needs to be validated. The material properties of the different body segments (organs, bones, cartilages, fat) are obtained from mechanical testing on sampled from PMHS for which there is some variability. The best validation data for the global response of the models are PMHS data. The following paragraphs will present the existing models ad well as their validation cases.

1.3.1.1 Presentation of the different models

This review covers the 50th percentile male models that have been developed until recently. Previous reviews of human body finite element models have been used for this purpose: Yang et al. 2006, Labé 2008, Lamielle 2008 and Luet 2013.

The first model of the human abdomen including different parts for the abdomen cavity is the LAB [16] model as detailed in Lizee et al. 1998. As it can be seen on Figure 1.19c the abdomen was divided in only three solid parts. Further improvements of the model have been mentioned in Luet 2013.

The WSUHAM [17] model is detailed in Lee and Yang 2001. This model is limited to the abdomen region only as it can be seen on Figure 1.19d. It has however been enhanced in Shah et al. 2004 to become a full-body model.

The HUMOS [18] model has been developed as a joint project by the HUMOS consortium. The model has been detailed in Robin 2001 and an improved version, HUMOS 2 in Vezin and Verriest 2005. Figure 1.19e shows the HUMOS 2 model.

A full human body model has been developed by Ford Motor Company and detailed in Ruan et al. 2003. Figure 1.19g shows a full model view as well as an abdomen view of the model.

A full human body model has been developed by Takata company and mentioned in Zhao and Narwani 2005. It gathers together previous models developed by Wayne State University for the thorax, abdomen, shoulder and head-neck regions. This model has been further improved as mentioned in Zhao and Narwani 2007. Figure 1.19i shows the first version of the model.

From this point, highly detailed models of the internal organs of the abdomen have been developed. The first of those models, limited to the abdomen, has been developed in Labé 2008 as seen on Figure 1.19j. The model has been further improved in Chebil 2014.

Then the THUMS model with detailed internal organs have been released and described in Shigeta et al. 2009 (see Figure 1.19o). The previous version of the THUMS model can be seen on Figure 1.19m. This model has been described in Iwamoto et al. 2003.

16. Laboratoire d'Accidentologie et de Biomécanique
17. Wayne State University model of the Human AbdoMen
18. HUman MOdel for Safety

The most recent full body model is the GHBMC [19] model. It has been developed by a consortium of automotive manufacturers and universities. The model has a highly detailed abdominal region as can be seen on Figure 1.19k. The model is detailed in Gayzik et al. 2012.

19. Global Human Body Models Consortium

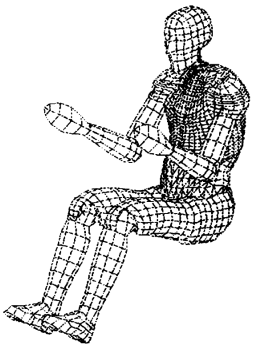

(a) LAB full model (Lizee et al. 1998)

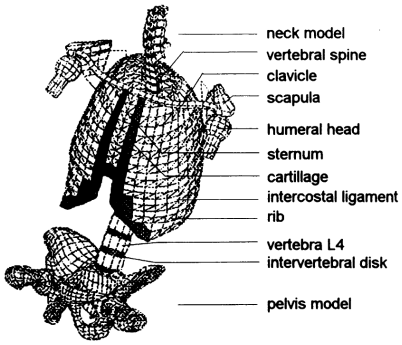

(b) LAB model thorax (Lizee et al. 1998)

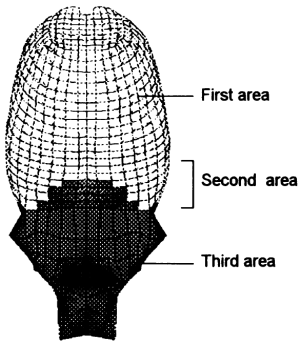

(c) LAB model abdomen (Lizee et al. 1998)

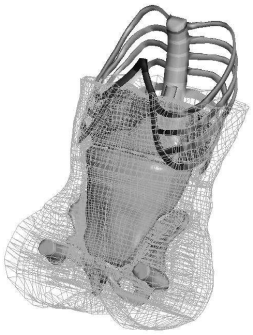

(d) WSUHAM model (Lee and Yang 2001)

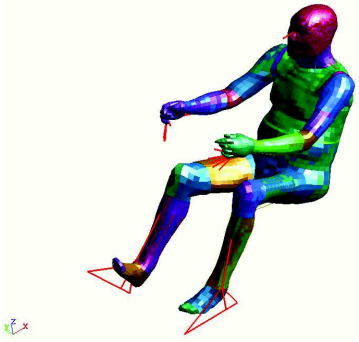

(e) HUMOS 2 full model (Vezin and Verriest 2005)

(f) HUMOS 2 abdomen (picture from Lamielle 2008)

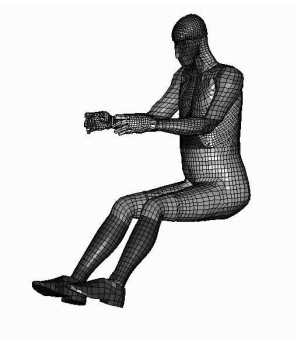

(g) Ford model (Ruan et al. 2003)

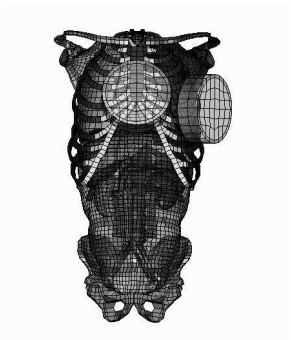

(h) Ford model abdomen (Ruan et al. 2003)

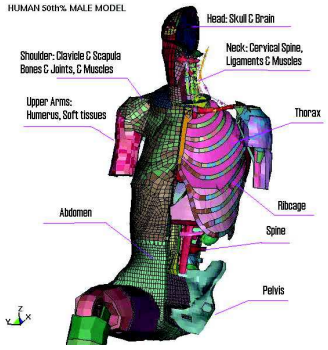

(i) Takata model (Zhao and Narwani 2005)

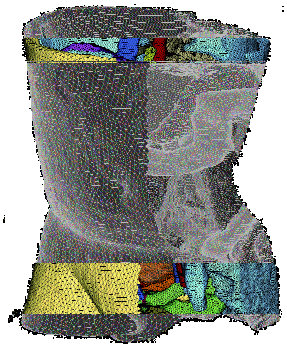

(j) Abdomen model from Labé 2008

(k) GHBMC full model (Gayzik et al. 2012)

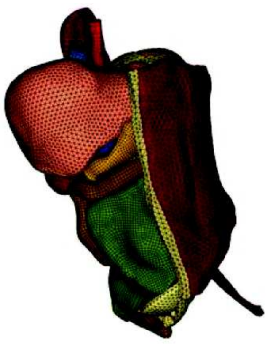

(l) GHBMC model abdomen (Gayzik et al. 2012)

Figure 1.19 – Overview of finite element human body models

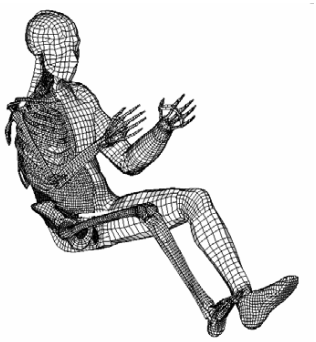

(m) THUMS model from Iwamoto et al. 2003

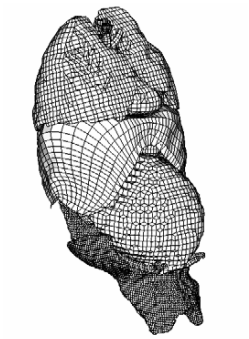

(n) THUMS model abdomen from Iwamoto et al. 2003

(o) THUMS model from Shigeta et al. 2009

(p) THUMS model abdomen from Shigeta et al. 2009

Figure 1.19 – Overview of finite element human body models (continued)

1.3.1.2 Comparison of the model responses

The above-mentioned models of the human abdomen have been validated against numerous tests described in the literature. Only frontal impacts test conditions will be reported here, according to the conditions described in the previous section.

Figures 1.20 shows the response of the models under the impact test described in Cavanaugh et al. 1986. The corridors from Lebarbé et al. 2015 are overlaid to the model responses. Different impactor masses and impact velocities were used to validate the different models. Figure 1.21 shows the responses if some models under the impactor test described in Hardy et al. 2001. The impactor mass was 48 kg for this test. The corridor defined as standard deviation boundaries versus mean penetration from PMHS tests was plotted.

Data for the validation of the HUMOS model were taken from Haug et al. 2004. The response of the model to a 32 kg 6.1 $\mathrm{m\,s^{-1}}$ can be seen on Figure 1.20a.

The WSUHAM has been validated against impactor tests in Lee and Yang 2001. Four conditions at different impact velocities and impactor masses were performed and can be seen on Figure 1.20.

The validation of the Ford model has been described in Ruan et al. 2005. Three actual impact conditions from Cavanaugh et al. 1986 were performed, simulating tests 24, 41 and 57. The velocities are reported on the plots legends of Figure 1.20. The impactor masses were not exactly 32 kg and 64 kg but those values have been rounded for clarity. Two tests from Hardy et al. 2001 (GI6 and GI8) were also simulated. The mass of the impactor was 48 kg and the velocities values are reported on Figure 1.21.

Impactor validation of the Takata model has been performed in Zhao and Narwani 2005 against the

condition described in Cavanaugh et al. 1986 (Figure 1.20a) and against the condition from Hardy et al. 2001 (Figure 1.21).

The abdomen-only model from Labé 2008 has been subjected to two conditions from Cavanaugh et al. 1986. Two impact velocities were used, corresponding to two different impactor masses. The masses were not exactly 32 kg and 64 kg but the values have been rounded for clarity. The model responses can be seen on Figures 1.20a and 1.20c.

The first version of the THUMS model has been subjected to a 32 kg $10.4\,\mathrm{m\,s^{-1}}$ as seen on Figure 1.20b. This has been reported in Iwamoto et al. 2002. The latest version of the model faced in Shigeta et al. 2009 an impact from Cavanaugh et al. 1986 as reported on Figure 1.20a.

The GHBMC model response has been compared to several impact cases in Beillas and Berthet 2012 under a $6\,\mathrm{m\,s^{-1}}$ impact from Hardy et al. 2001 and is presented on Figure 1.21.

Fewer models have been validated under seatbelt tests than under impactor tests. The reasons for this are the difficulties to reproduce the input conditions of the tests performed on PMHS in the literature and the challenge for the models to show a biofidelic behaviour at rapidly changing strain rates. Figure 1.22 shows the model responses. The corridor defined as standard deviation boundaries versus mean penetration from PMHS tests was plotted with no normalisation, since Lebarbé et al. 2015 reported that no normalisation method was suited to seatbelt loadings.

In Shah et al. 2004, a seatbelt test condition from Hardy et al. 2001 was reproduced on the WSUHAM model. A time-velocity profile from test data (motion of the ram pulling the belt) was applied to the belt of the model. The response of the model can be seen on Figure 1.22a.

The Ford model has been submitted to the configuration from Hardy et al. 2001 as detailed in Ruan et al. 2005. It is presumable that the belt velocity was applied although it is not mentioned. In Rouhana et al. 2010, the force profile (with some modifications) from Foster et al. 2006 A2 test was applied on the belt of the model. The response of the model to those tests can be seen on Figures 1.22a and 1.22b.

Figure 1.22a shows the response of the Takata model to the condition from Hardy et al. 2001 as described in Zhao and Narwani 2005. It is not detailed which quantity from the test data was applied to the seatbelt in the simulation.

The THUMS model has been subjected to the seatbelt A condition test from Foster et al. 2006. The belt was pulled with a maximum velocity of $6.9\,\mathrm{m\,s^{-1}}$. The result of this test is displayed on Figure 1.22b.

All the presented models were correctly representing the stiffness of the PMHS data under impactor loading, including rate-sensitivity. For the low velocity condition from Cavanaugh et al. 1986 (Figure 1.20a), the models tend to predict a stiffness in the higher part of the corridor and to be out of the corridor after a certain penetration. The model from Labé 2008 has a higher stiffness than the corridor bounds. This can be due to the fact that PMHS responses from subject impacted at different velocities were used to create the corridor. For the models submitted to the Hardy et al. 2001 conditions, the models responses are also on the upper part of the corridor for the $6\,\mathrm{m\,s^{-1}}$ condition. This can be explained by the fact that the corridor presented was non normalised and that the PMHS have abdomen depths from 29 cm to 31 cm. The 50th percentile male abdomen depth being 26 cm (Schneider et al. 1989), a normalised comparison in terms of abdomen depth would bring the model and PMHS curves closer.

Under seatbelt loading condition, the model responses are close to the corridors for both conditions (Figure 1.22), except for the Ford model which presents a lower stiffness.

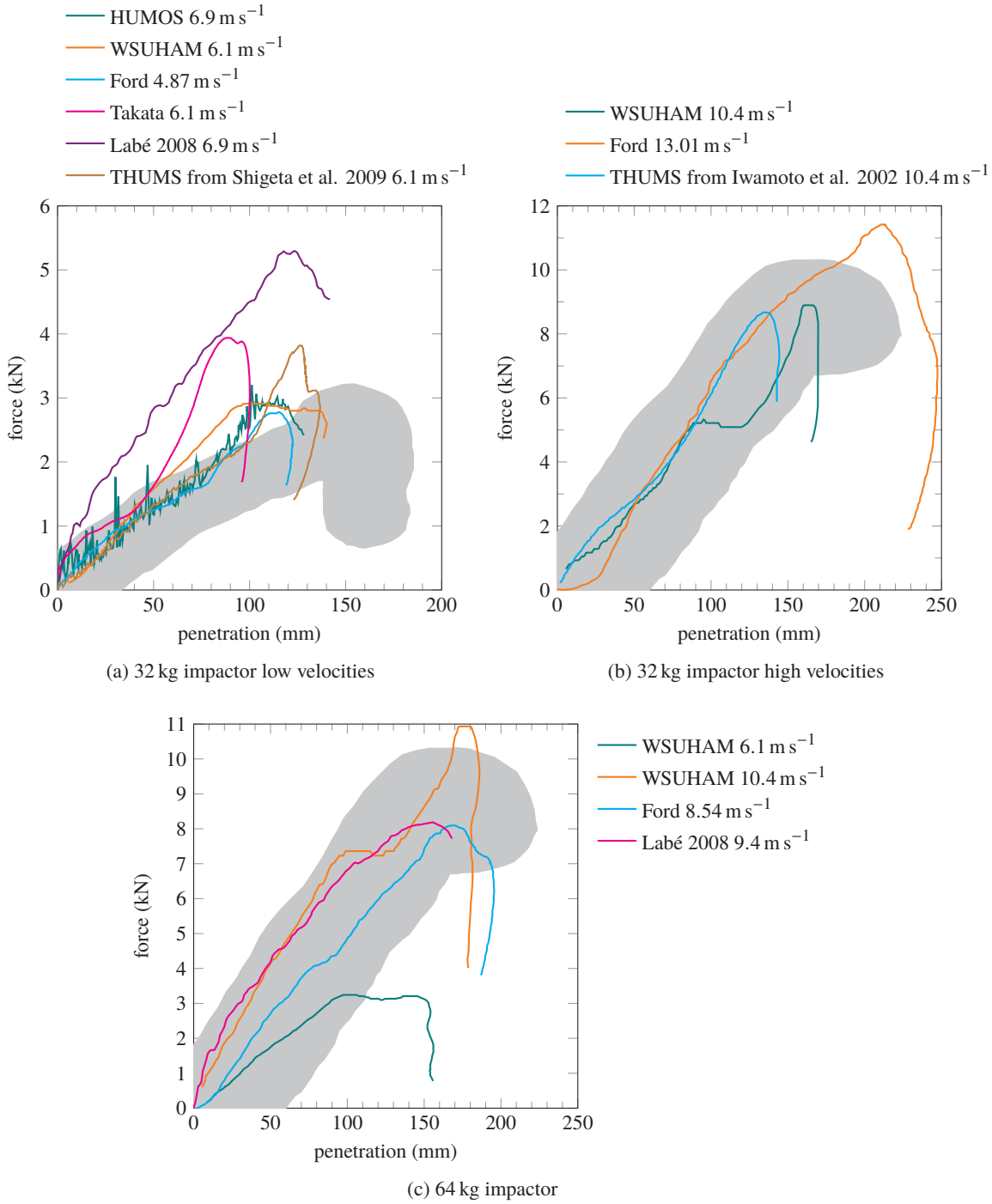

(a) 32 kg impactor low velocities

(b) 32 kg impactor high velocities

(c) 64 kg impactor

Figure 1.20 – Finite element models responses under Cavanaugh et al. 1986 impactor test

The mass of the impactor used in the test is mentioned in each subfigure caption and the impact velocity is specified in the plot legend

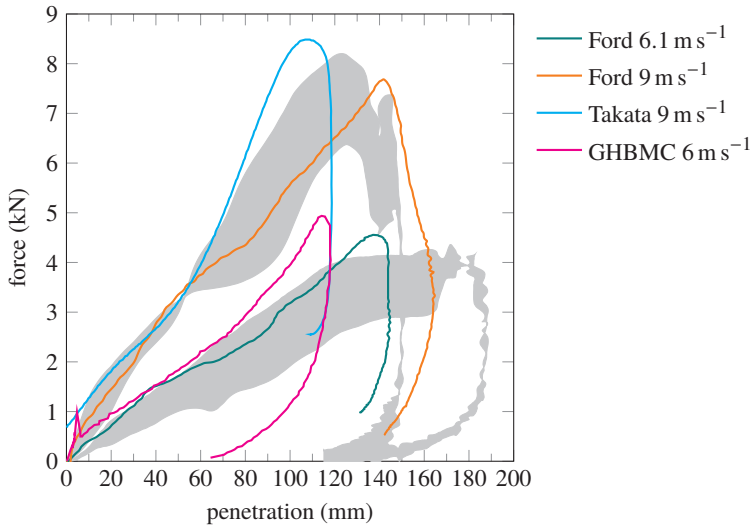

Figure 1.21 – Finite element models responses under Hardy et al. 2001 lower-abdomen impactor test
The impact velocity for each test is specified in the plot legend
Corridors are non-normalised

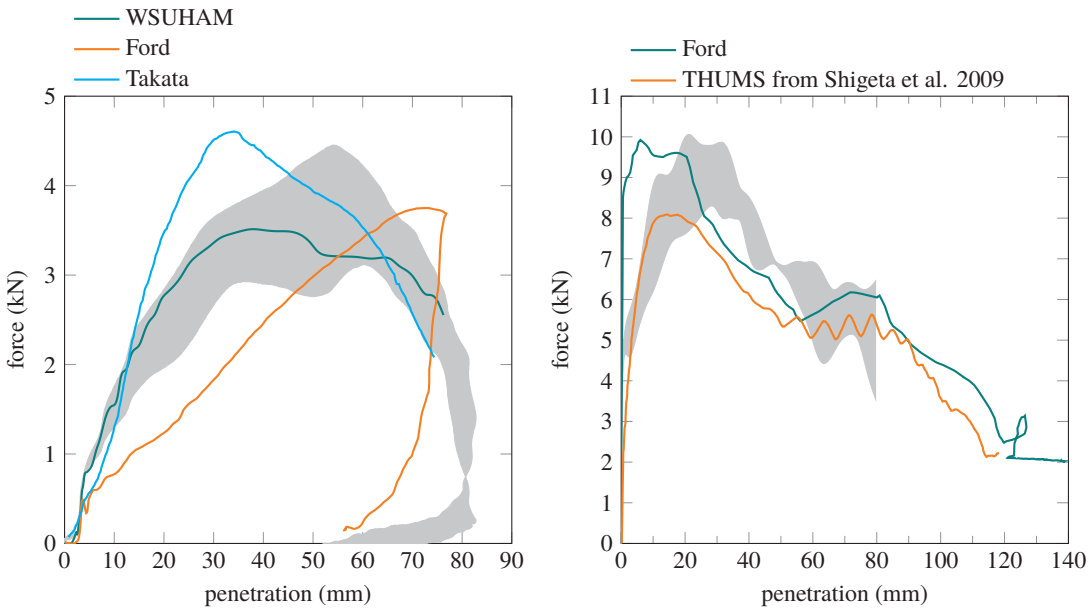

(a) Hardy et al. 2001 seatbelt test

(b) Foster et al. 2006 seatbelt test

Figure 1.22 – Finite element models responses under seatbelt tests
Corridors are non-normalised

1.3.1.3 Injury prediction

So far, finite element human body models have been used for injury prediction by looking at maximum values of local variables such as stress or strain in specified organs. Shigeta et al. 2009 mentioned a 30 % value for first principal strain for solid organs (liver) and 120 % for hollow organs (stomach, intestine) as maximum acceptable value before injury. Figure 1.23a shows injury prediction results for the THUMS model under an impactor test condition (Cavanaugh et al. 1986). However, although most of the intestine properties for the THUMS model were taken from Yamada 1970, the reference strain value used were not documented. First principal strain was also the indicator used in Kitagawa and Yasuki 2013 and was found to be correlated with ribcage deflections only for the spleen. Figure 1.23b shows the strain values for the organs of the THUMS model for a frontal collision simulation. However, no validation of the internal behaviour of finite element models of the human body have been carried on so far. For instance, PMHS tests with markers placed in the organs and imaged by X-ray have been performed in Howes et al. 2012 and Howes et al. 2015. Beillas et al. 2013 performed impact tests on PMHS with an impactor containing an ultrasound probe and another probe was placed on the opposite side of the subject, both linked to an ultrafast data acquisition system and imaging the internal organs. These new experimental protocols allowing to monitor the internal motion of organs during an impact test could give reference data for internal model validation.

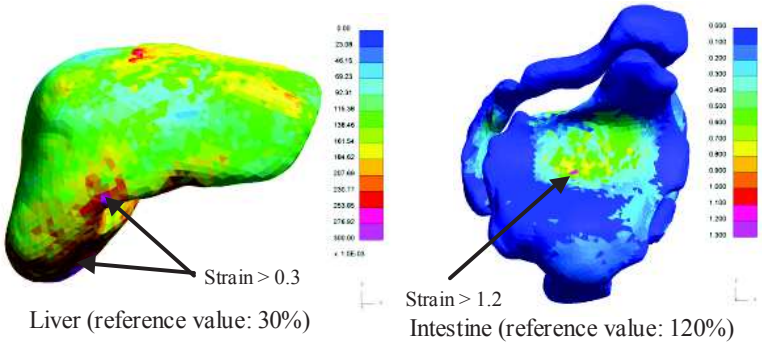

(a) Shigeta et al. 2009

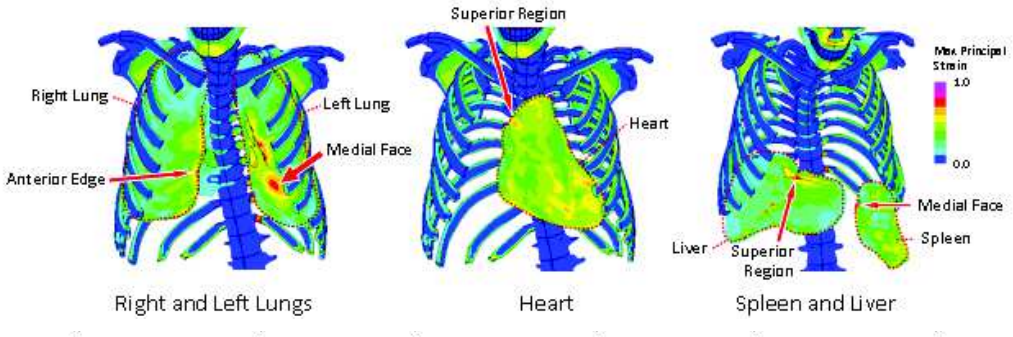

(b) Kitagawa and Yasuki 2013

Figure 1.23 – Injury prediction with the THUMS model

The new generation of human body finite element models with detailed description of the internal structure of the human abdomen is validated against PMHS test data but not yet regarding internal organs displacement or internal organ pressure. However, the fact that these models include a detailed anatomical representation of the abdomen organs as well as specific material data for each organ should allow them to be used for injury prediction on a global scale such as a group of organs or a region of the abdomen.

1.3.2 Crash test dummies

1.3.2.1 Overview of frontal impact dummies

The current regulatory dummy is the Hybrid III, first desbribed in Foster et al. 1977. It was not equipped with an instrumented abdomen. The standard abdomen was made of foam enclosed in a vinyl coating and was not linked to the rest of the body but only inserted in the gap between the thorax and the pelvis. This abdomen can be seen on Figure 1.24a.

The THOR dummy was originally a new torso (Schneider et al. 1992; Haffner et al. 1994) for the Hybrid III dummy called TAD-50M [20]. The TAD-50M has evolved to THOR Alpha (Haffner et al. 2001), then to THOR NT (Shams et al. 2005) and finally to THOR Mod-kit (Ridella and Parent 2011). The abdomen of the THOR dummy is made of two foam block of different stiffnesses and is instrumented with deflection sensors.

Figure 1.24 shows the anatomical difference between the Hybrid III and THOR. For instance, the THOR dummy has one more ribs (seven instead of six) than Hybrid III, representing better the human anatomy consisting of ten ribs.

(a) Hybrid III (b) THOR

Figure 1.24 – Anatomy comparison between Hybrid III and the THOR dummy (Shaw et al. 2004)

1.3.2.2 Previous abdomen concepts

Since the Hybrid III did not have an instrumented abdomen, a frangible abdomen had been proposed in Rouhana et al. 1989 to detect submarining and have an history of the penetration sustained abdomen (Figure 1.25a). A first instrumented abdomen made of elastic foam rubber has been developed in Ishiyama et al. 1994 along with a measurement system called TADAS [21] that measures the contour variation of the abdomen (Figure 1.25b). More recently, Rouhana et al. 2001 designed a rate-sensitive abdomen with improved biofidelity for the Hybrid III. This abdomen consisted in a silicone rubber shell filled with silicone gel. It incorporated a deflection measurement system based on electrical resistance (Figure 1.25c).

The design of an instrumented abdomen for the THOR dummy has been described in Rangarajan et al. 1996 and Rangarajan et al. 1998. This design has been used for the Alpha, NT and Mod-kit versions. It is composed of two foam block attached at the back to a plate, itself attached to the spine

20. Trauma Assessment Device 50th percentile male
21. Toyota Abdominal Deformation Analyzing System

of the dummy. The foam block and the plate are placed inside a fabric bag. Telescopic deflection sensors are attached to the plate brackets and go through the foam blocks. The original sensors were DGSP [22] sensors until the Mod-kit version where IRTRACC [23] sensors were implemented for the same purpose. Figures 1.25d and 1.25e shows the abdomen parts and assembly.

An alternative to the THOR NT dummy called THOR FT has been developed and included a different abdomen design as well as a pelvis modification. This abdomen was made of a single foam block enclosed in a vinyl skin layer and was equipped with IRTRACC sensors. The lower abdomen response of the FT dummy was very similar to the NT response according to Onda et al. 2006. Figure 1.25f shows the THOR FT abdomen and Figures 1.25g and 1.25h compre the pelvis for the two dummy versions.

An abdomen for the THOR dummy designed by GESAC and Toyota Motor Corporation have been mentioned in Hanen et al. 2011 (Figure 1.25i). This abdomen consists in a urethane core moulded around three metal weights (of approximately 250 g) and enclosed in a urethane shell. The total weight of the insert is 3.6 kg. This abdomen proved to have a really stiff response compared to biofidelity corridors.

22. Double Gimbaled String Potentiometer
23. Infra Red Telescoping Rod for the Assessment of Chest Compression

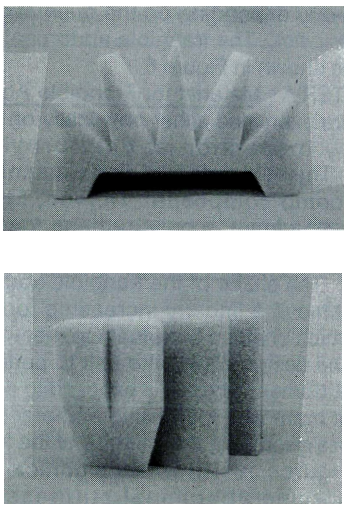

(a) Frangible abdomen for the Hybrid III (Rouhana et al. 1989)

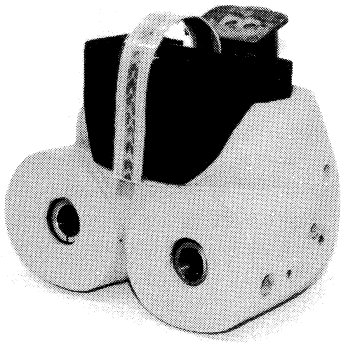

(b) Abdomen from Ishiyama et al. 1994 for the Hybrid III

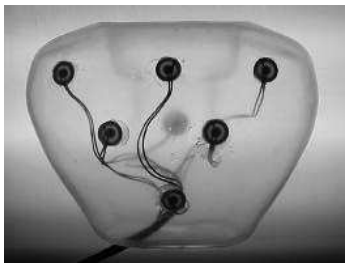

(c) Rate-sensitive abdomen for the Hybrid III (Rouhana et al. 2001)

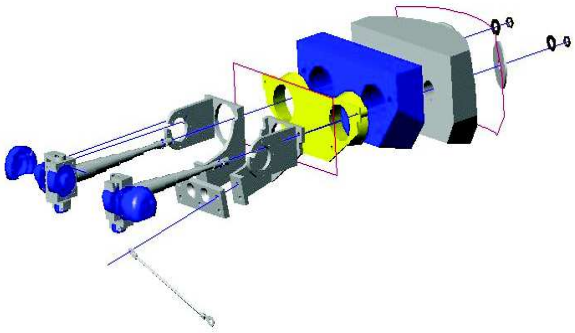

(d) THOR abdomen exploded view (THOR NT Manual, NHTSA / GESAC, Inc. 2005b)

(e) THOR abdomen assembly view (THOR NT Manual, NHTSA / GESAC, Inc. 2005b)

(f) THOR FT abdomen (Onda et al. 2006)

(g) THOR FT pelvis (Onda et al. 2006)

(h) THOR NT pelvis (Onda et al. 2006)

(i) GESAC / Toyota abdomen (Hanen et al. 2011)

(j) IFSTTAR / Toyota prototype abdomen

Figure 1.25 – Abdomen concepts for Hybrid III and THOR dummies

1.3.2.3 IFSTTAR / Toyota prototype abdomen

Based on all the existing dummy abdomen concepts, the need for an abdomen equipped with an omni-directional measurement and with improved biofidelity appears. The abdomen from Rouhana et al. 2001 showed acceptable biofidelity but problems were reported with the measurement system. Furthermore, this abdomen was designed for the Hybrid III dummy, and therefore is not attached to others dummy elements but just inserted between the ribcage and the pelvis.

This led to the development of the last prototype abdomen for the THOR dummy that was developed by IFSTTAR and Toyota Motor Europe and described in Compigne et al. 2015. Figure 1.25j shows the prototype mounted on the dummy. It includes in the standard THOR abdomen two APTS pressure sensors (presented in Beillas et al. 2012) and additional steel masses in order to add 825 g at the front of the abdomen. The biofidelity of IFSTTAR / Toyota prototype abdomen has been evaluated in Compigne et al. 2015 under impactor and seatbelt loading conditions, respectively under Cavanaugh et al. 1986 6.1 m s^{-1} impact and Foster et al. 2006 seatbelt loading with pretensioners (B condition). Figure 1.26 shows the response curves overlaid with the respective PMHS corridors. The prototype has a closer response to the PMHS data under the impactor loading due to a decreased stiffness after the characteristic inflexion in the force-penetration diagram. The biofidelity is also improved under seatbelt loading due to a higher inertia created by the additional masses creating the initial force peak.

The IFSTTAR / Toyota abdomen has therefore an acceptable biofidelity and an adequate measurement system. It can therefore be used for discriminating injurious loadings based on the pressure measurements of the APTS sensors, if a specific injury criteria is developed.

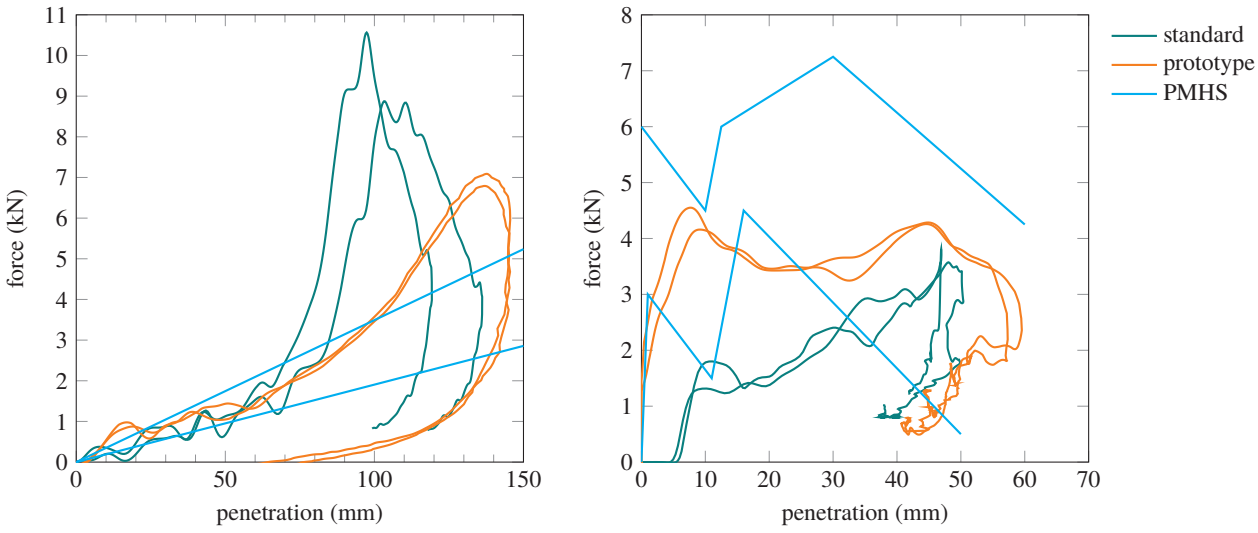

(a) Cavanaugh et al. 1986 impactor condition

(b) Foster et al. 2006 B seatbelt condition

Figure 1.26 – Biofidelity evaluation of IFSTTAR / Toyota prototype abdomen (Compigne et al. 2015)

1.4 Conclusion and objectives of this thesis

There is a global need to decrease the number of road fatalities, frontal impact being the most common crash case. The abdomen is a crucial region regarding serious to critical injuries, especially for rear passengers and in case of submarining. However, no injury criterion for the abdomen is applied in the regulation or by consumers organisations. The THOR dummy is planned to become the future dummy used in regulation and consumers tests but the biofidelity of its abdomen needs to be improved and its sensors measurement needs to be linked to an injury risk. The recent abdomen prototype developed by IFSTTAR and Toyota has shown better biofidelity than the standard abdomen and has the ability to estimate omni-directional loading severity thanks to APTS sensors. Furthermore, recently developed finite element models of the human body having a highly detailed geometry of the abdominal organs will allow for injury prediction on a regional level based on engineering parameters obtained from impact simulations.

The aim of this work is to improve the biofidelity of the IFSTTAR / Toyota prototype through finite element modelling, to evaluate its influence on the global dummy behaviour and to develop an injury criteria based on abdominal sensors pressure measurements.